Archive of Applied Mechanics (2023) 93:4467–4496
https://doi.org/10.1007/s00419-023-02504-2

ORIGINAL

Raj Kumar · Prasun Jana

Dynamic stiffness method for exact modal analysis of sigmoid functionally graded rectangular plate resting on elastic foundation

Received: 17 May 2023 / Accepted: 4 October 2023 / Published online: 30 October 2023

Abstract The present paper deals with the modal analysis of sigmoid functionally graded (S-FGM) rectangular plate resting on elastic foundation by using the dynamic stiffness method (DSM). The DSM is formulated based on the exact solutions of the governing differential equations, and thereby it results in the very accurate computation of the natural frequencies. To obtain the DSM results for thicker plates, the study incorporates first-order shear deformation theory (FSDT) which includes the important effects of transverse shear deformation and rotatory inertia. The governing equations and the associated natural boundary conditions are derived using Hamilton's principle, and the solution is sought in the Levy form where two opposite edges of the plate are simply supported. The present study also contributes by highlighting mistakes in the classical plate theory (CPT)-based DSM formulation published in a recent work and presents a correct CPT-based mathematical formulation. For both these cases, the frequency-dependent dynamic stiffness matrix of the S-FGM plate gives rise to the transcendental eigenvalue problem, which is solved by using the Wittrick and Williams algorithm. Comparison with the available literature establishes the accuracy of the method. In addition, a parametric study is presented for various geometric and stiffness parameters of the elastically supported S-FGM plates using both CPT- and FSDT-based formulations, and accurate frequency results are reported.

Keywords Free vibration · S-FGM plate · Elastic foundation · Classical plate theory · First-order shear deformation theory · Dynamic stiffness method

1 Introduction

The paper focuses on the exact modal analysis of a sigmoid functionally graded (S-FGM) rectangular plate resting on Winkler–Pasternak foundation by using the dynamic stiffness method (DSM). The present study is of practical relevance as the functionally graded material is now considered to be an advanced class of material used mainly in the design of structural components that are subjected to thermo-mechanical loads. In the design of weight-sensitive structures in aerospace, naval, automotive, and other allied industries, the use of both laminated composite material and functionally graded materials is almost inevitable as they provide superior strength and stiffness properties in comparison with other conventional materials. However, laminated structures often experience issues related to debonding and the development of residual stresses at the interfaces, which eventually leads to the initiation of cracks within the material. To overcome the issue of debonding, the idea of functionally graded material (FGM) had been conceived [1]. In general, FGM plates are produced

R. Kumar · P. Jana (✉)
Department of Aerospace Engineering, Indian Institute of Technology, Kharagpur, Kharagpur, West Bengal 721302, India
E-mail: prasunjana@gmail.com; prasun@aero.iitkgp.ac.in

R. Kumar
E-mail: rajme0927@gmail.com; rajaero@iitkgp.ac.in

by proper mixing of metal and ceramic constituents, effectively eliminating the concept of discrete layers in laminates [2], which eventually produces a smooth variation of mechanical properties along the preferred direction [3,4]. The metal constituents possess superior strength and fracture resistance, whereas ceramic constituents provide high thermal resistance [5]. Furthermore, it offers the added benefit of tailoring the material properties for specific requirements [6]. Due to superior mechanical, electrical, and thermal properties over traditional materials, the structures made of functionally graded material have found their usages in many industrial applications [7]. When operated in external environments, these FGM structures are subjected to severe conditions resulting in excessive noise and vibration. Therefore, the vibration characteristics of FGM materials must be thoroughly studied in order to design the structure properly.

Several micromechanical models based on power-law function (P-FGM) [8–11], sigmoid function (S-FGM) [12–14], and exponential function (E-FGM) [15,16] are proposed for the estimation of spatial distribution of material constituents along the thickness direction of the FGM plate. Based on these mathematical functions, the effective material properties are determined. A thorough literature study reveals that the static and dynamic analysis of FGM plates based on the power-law micromechanical model is quite significant in number, whereas very few literature are available that carried out the analysis of FGM plate based on the sigmoid micromechanical model. In the sigmoid micromechanical model, the volume fraction is defined using two power-law functions, one from the middle surface to the top surface and other from the bottom surface to the middle surface. The separate functions for the distribution of the volume fraction in each half of the plate ensure the smooth distribution of interfacial stresses and make it more applicable for layered FGM [17] structures. Note that a study of free vibration behavior of S-FGM plate using a classical plate theory (CPT)-based dynamic stiffness method has been attempted by Chauhan et al. in their recent paper [18]. However, a careful analysis reveals that the formulation presented in that paper is inappropriate and the reported numerical results for S-FGM plates are incorrect. In this context, the main objectives of the present study are twofold: (i) To highlight possible mistakes in the CPT-based dynamic stiffness (DS) formulation in recent work of Chauhan et al. [18], and (ii) to present correct results using the dynamic stiffness formulations based on both CPT and FSDT, i.e., the higher-order shear deformation theory. Using the FSDT, the present work advances the previously published work [18], which includes the DS matrix formulation applicable to thicker S-FGM plates by incorporating the important effects of transverse shear deformation and rotatory inertia.

Therefore, the main focus of the present study is to study the free vibration analysis of the S-FGM plate resting on the Winkler–Pasternak foundation using both CPT- and FSDT-based dynamic stiffness method. Plates resting on elastic foundations have been used in many structural applications ranging from railroad tracks to nuclear reactors. Initially, a Winkler model for railroad interaction was developed to investigate the effect of underlying layers on plate vibration. In this model, several independent and unconnected springs are placed beneath the structure to study the effect of elastic foundation [19,20]. However, the Winkler model does not represent a realistic situation because of the independent and unconnected springs. Later, in Pasternak model a shear layer is introduced to accommodate the longitudinal and lateral displacement of springs [21,22]. In recent times, the plate supported by the Winkler–Pasternak foundation increasingly found its application in foundation engineering. Several researchers carried out the static and dynamic analysis of isotropic and orthotropic plates resting on Winkler–Pasternak foundation. Xiang [23] presented the closed-form solution of the pre-stressed simply supported plate resting on elastic foundation. Lam et al. [24] analyzed the static and dynamic behavior of the plate using the Green function. Malekzadeh et al. [25] analyzed the free vibration of plate, having continuous thickness variation and supported on a two-parameter foundation, using a FSDT-based differential quadrature method. Baferani et al. [26] employed an analytical method for the free vibration analysis of P-FGM plate based on third-order shear deformation theory. Jung et al. [27] presented a refined higher-order shear deformation theory to analyze the vibration behavior of S-FGM plate resting on elastic foundation. There are several other studies available in the literature which deal with the vibration analysis of plates resting on elastic foundations. However, a careful survey of the past works reveals that a majority of these works adopted different numerical methods such as the finite element method and the finite strip method [28–30] for studying the static and dynamic behavior of elastically supported plates. It must be noted that these numerical methods require a large mesh size for the convergence of solutions, which in turn increases the computational cost. Furthermore, these methods provide an approximate solution, especially at higher frequencies, due to several assumptions made en route to the solution. On the contrary, the dynamic stiffness method can be adopted as a solution methodology to obtain very accurate solutions with reasonable computational time [31–34] and this method is the primary focus of the present work. DSM utilizes the closed-form solutions of the governing differential equation while maintaining the accuracy and exactness of the result as opposed to FEM [35,36].

In a nutshell, this study presents an exact dynamic stiffness matrix formulations based on both CPT and FSDT and discusses the free vibration results for the elastically supported S-FGM plates in detail. The dynamic stiffness matrix is derived for a Levy-type plate, where two opposite edges are simply supported. It must be noted here that the CPT-based DS matrix formulation presented in the recent work of Chauhan et al. [18] is inappropriate, and it leads to incorrect frequency results for the S-FGM plates resting on elastic foundations. Therefore, the present work should be treated as a correction to the work of Chauhan et al. [18] to apply the dynamic stiffness method for the free vibration analysis of elastically supported S-FGM plates. Over and above, the present study further enriches the existing literature by introducing a FSDT-based dynamic stiffness formulation, for the elastically supported S-FGM plates, which has broader applications than the CPT-based formulation. Thus, the novelty of the present study lies in presenting, first time in the literature, mathematically correct dynamic stiffness formulations based on both CPT and FSDT for the free vibration analysis of FGM plates resting on Winkler–Pasternak elastic foundation. By implementing the exact DSM formulations, very accurate frequency results are obtained for various values of geometric and stiffness parameters of the elastically supported FGM plates and these results can serve as benchmark for any future comparative studies.

2 Scope and contributions of the present work

As discussed earlier, in this work, exact dynamic stiffness formulations based on both CPT and FSDT are presented for the free vibration analysis of S-FGM plate resting on Winkler–Pasternak foundation. The governing differential equations and the boundary conditions are derived using Hamilton's principle. Assuming Levy-type BCs, a system of linear differential equations is obtained, which leads to the formation of the dynamic stiffness matrix for a plate element. These element stiffness matrices are properly assembled to form the frequency-dependent global dynamic stiffness matrix, which is solved by employing well-known Wittrick–Williams algorithm [37,38]. Based on the feature of the Sturm sequence, the Wittrick–Williams algorithm makes sure that all the natural frequencies within a given frequency range are computed without missing any single frequency. Using this DSM approach, parametric studies have been carried out to obtain the natural frequencies of S-FGM plate resting on elastic foundation by varying geometrical and stiffness parameters of the plate. In short, the key contributions of the present work can be listed as follows:

- For the first time in the literature, separate dynamic stiffness matrix formulations based on the kinematic variables of CPT and FSDT are presented for the S-FGM plate resting on Winkler–Pasternak foundation.
- Due to the transcendental nature of the dynamic stiffness matrix, Wittrick–Williams algorithm is employed in the present work for the accurate computation of natural frequencies for the elastically supported S-FGM plate.
- Some incorrect frequency results in the published literature [18] are highlighted. The possible reasons for the incorrectness are also discussed in detail.
- New set of results are obtained for both uniform and non-uniform S-FGM plate resting on elastic foundation by varying different plate parameters and elastic foundation coefficients. These results are presented in both tabulated and graphical forms, and a number of important conclusions are drawn.

With this note, the mathematical details for the DSM formulation are presented below for the vibration analysis of S-FGM plate resting on elastic foundation.

3 Materials and method

In this section, material property variations within the S-FGM plate are described followed by the detailed mathematical formulation for both CPT- and FSDT-based dynamic stiffness approach.

3.1 The plate geometry and the material property description

The length, width, and thickness of the functionally graded rectangular plate element, as shown in Fig. 1, are L, b, and h, respectively. As mentioned earlier, the functionally graded materials are made up by varying volume fraction of the material constituents along the thickness direction which also causes change in mechanical properties of the plate. In this study, the idealized mathematical model termed as sigmoid law (S-FGM) has been used to describe the variation of material properties in the thickness direction of the plate.

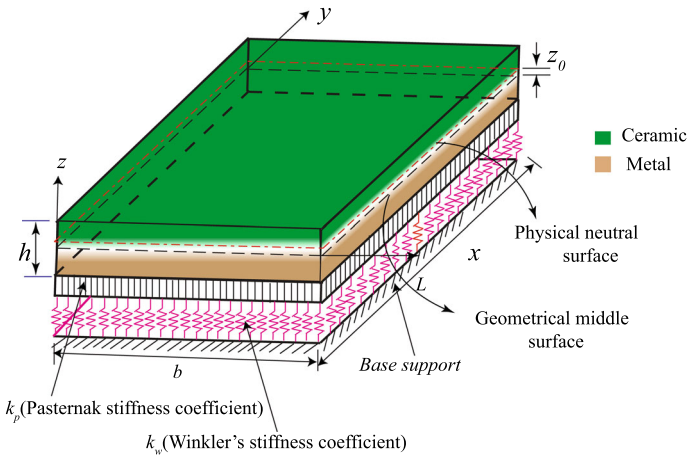

Fig. 1 A functionally graded rectangular plate element supported on elastic foundation showing both the geometric midsurface and the physical neutral surface

The volume fractions of the material constituents along the thickness direction in S-FGM plate are defined as:

$$\begin{aligned} V_t(z) &= 1 - \tfrac{1}{2}\left(\tfrac{h-2z}{h}\right)^p; \quad \text{for } 0 \le z \le h/2 \\ V_b(z) &= \tfrac{1}{2}\left(\tfrac{h+2z}{h}\right)^p; \quad \text{for } -h/2 \le z \le 0 \end{aligned} \tag{1}$$

Here, $0 \le p \le \infty$ is a parameter, known as sigmoid-function exponent (or sigmoid volume fraction index), and determines the proportion of ceramic and metal in the thickness direction of the plate. The material constituents vary as one proceeds from bottom to top of the plate. As a function of z-coordinate, the equivalent material properties are calculated using the rule of mixture:

$$\begin{aligned} X_1(z) &= V_t(z)X_c + [1 - V_t(z)]X_m; \quad \text{for } 0 \le z \le h/2 \\ X_2(z) &= V_b(z)X_c + [1 - V_b(z)]X_m; \quad \text{for } -h/2 \le z \le 0 \end{aligned} \tag{2}$$

Here, X_c and X_m refer to the material property (e.g., Young's modulus (E), density (ρ), Poisson's ratio (μ), etc.) values of the pure ceramic and pure metal, respectively. Interestingly, the behavior of the plate changes from homogeneous isotropic to bimetallic plate as the value of p increases from 0 to ∞. The homogeneous isotropic plate will take the average property of the material constituents, whereas the bimetallic plate consists of ceramic constituent at the top half and metallic counterparts at the bottom half.

3.2 Governing equations derivation

Hamilton's principle is used for the derivation of the governing equations and the natural BCs, which is expressed as:

$$\delta \int_{t_1}^{t_2} (T - P - V_{ef})\mathrm{d}t = 0. \tag{3}$$

Here, T stands for the kinetic energy and expressed as

$$T = \frac{1}{2}\int_A \int_z \rho(\dot{u}^2 + \dot{v}^2 + \dot{w}^2)\mathrm{d}z\mathrm{d}A, \tag{4}$$

where ρ represents the equivalent mass density (see Eq. (2)) of the plate, and $(\cdot)$ denotes the time derivative. In Eq. (3), P denotes the potential energy which is expressed as

$$P = \frac{1}{2}\int_A \int_z \sigma^T \varepsilon \mathrm{d}z\mathrm{d}A, \tag{5}$$

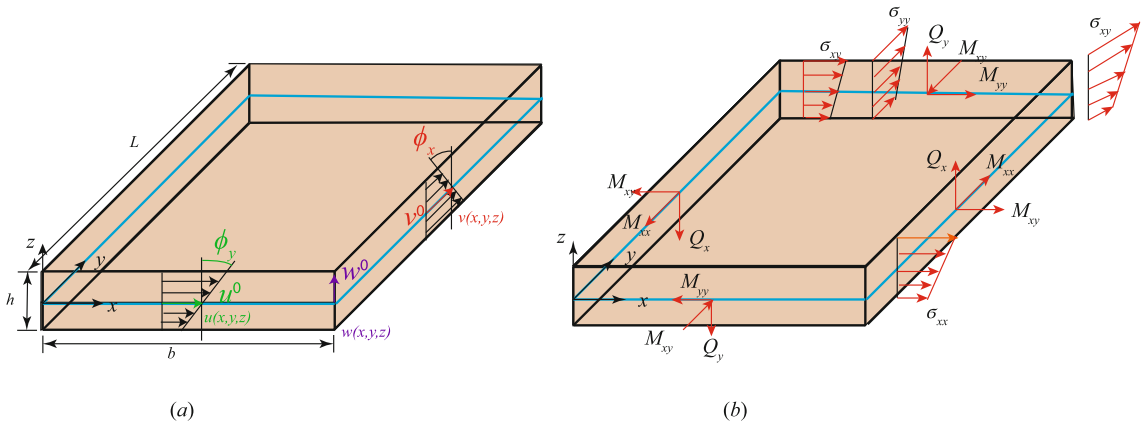

(*a*) (*b*)

Fig. 2 **a** Displacement field variable and rotation within the plate element. **b** Notation and the direction used for the forces and moments

where

$$\sigma^T = [\sigma_{xx}\ \sigma_{yy}\ \sigma_{xy}\ \sigma_{yz}\ \sigma_{xz}] \text{ and } \varepsilon^T = [\varepsilon_{xx}\ \varepsilon_{yy}\ \gamma_{xy}\ \gamma_{yz}\ \gamma_{xz}]. \tag{6}$$

The stress–strain constitutive relation used for the development of governing differential equation and natural boundary conditions is mentioned in Appendix A. In Eq. (3), V_{ef} represents the potential energy associated with the presence of elastic foundation and expressed as:

$$V_{ef} = \frac{1}{2}\int_A \int_z \left(k_w w^2 + k_p \left(\left(\frac{\partial w}{\partial x}\right)^2 + \left(\frac{\partial w}{\partial y}\right)^2 \right) \right) \mathrm{d}z\mathrm{d}A, \tag{7}$$

where k_w and k_p are the Winkler and Pasternak stiffness coefficients of the elastic foundation, respectively.

In the subsequent sections, the formulations considering the displacement field based on CPT and FSDT are discussed. First, the dynamic stiffness matrix is developed considering the kinematic variables according to CPT and subsequently for FSDT. Figure 2 shows the notations and sign conventions used for the displacement and force components within the plate in a Cartesian coordinate system. For mathematical simplicity, without compromising on the correctness of the method, the concept of physical neutral surface is used for defining the displacement components.

3.3 Concept of physical neutral surface

Due to the variation in the material stiffness along the thickness direction, the transverse motion and the in-plane displacements are, in general, coupled in FGM plate [39], which increases the complexity of the dynamic stiffness formulation. Abrate [40] observed that by aptly shifting the reference plane from plate's mid-surface to a new reference surface known as physical neutral surface [41], the stretching-bending coupling in the FGM plate can be avoided. The physical neutral surface position, defined by $z_{\text{pns}} = z - z_0$ [39], is determined by using the concept that the resultant force in the axial direction is zero. Here, z_0 is the distance between the plate's geometric mid-surface and the physical neutral surface (see Fig. 1). It can be shown that the net axial force will be zero when the first moment of the material stiffness (i.e., Young's modulus) about the reference surface is zero. Mathematically, we write

$$\int_{-h/2-z_0}^{h/2-z_0} z_{\text{pns}} E(z_{\text{pns}}) \mathrm{d}z_{\text{pns}} = \int_{-h/2}^{h/2} (z - z_0) E(z) \mathrm{d}z = 0, \tag{8}$$

which leads to,

$$\begin{aligned} z_0 &= \frac{\int_{-h/2}^{h/2} E(z) z \mathrm{d}z}{\int_{-h/2}^{h/2} E(z) \mathrm{d}z} = \frac{\int_0^{h/2} E_1(z) z \mathrm{d}z + \int_{-h/2}^{0} E_2(z) z \mathrm{d}z}{\int_0^{h/2} E_1(z) \mathrm{d}z + \int_{-h/2}^{0} E_2(z) \mathrm{d}z} \\ &= \frac{h(E_c - E_m)}{2(E_c + E_m)} \left[\frac{1}{2} - \frac{1}{(p+1)(p+2)} \right] \end{aligned} \tag{9}$$

3.4 Development of dynamic stiffness matrix based on classical plate theory (CPT)

Taking reference at the physical neutral surface, the displacement field based on the classical plate theory is expressed as:

$$\begin{aligned} u &= -z_{\text{pns}}\frac{\partial w_0}{\partial x} &&= -(z-z_0)\frac{\partial w_0}{\partial x} \\ v &= -z_{\text{pns}}\frac{\partial w_0}{\partial y} &&= -(z-z_0)\frac{\partial w_0}{\partial y} \\ w &= w_0(x,y,t) \end{aligned} \tag{10}$$

Applying the Hamilton's principle, as described in Sect. 3.2, the governing differential equation is developed for the S-FGM plate resting on elastic foundation as

$$D_{\text{sfgm}}(w_{0,xxxx}+2w_{0,xxyy}+w_{0,yyyy})+I_0\ddot{w}_0+k_w w_0-k_p(w_{0,xx}+w_{0,yy})=0 \tag{11}$$

The natural boundary conditions are:

$$\begin{aligned} V_x &: [-D_{\text{sfgm}}(w_{0,xxx}+(2-\mu)w_{0,xyy})+k_p w_{0,x}]\delta w \\ M_{xx} &: -D_{\text{sfgm}}(w_{0,xx}+\mu w_{0,yy})\delta\phi_y \end{aligned} \tag{12}$$

Here, D_{sfgm} is the flexural rigidity, and I_0 is the transverse inertia of the S-FGM plate and their expressions are given in Appendix B.

The solution which satisfies the simply supported BCs at $y=0$ and $y=L$ is given by:

$$w_0(x,y,t)=\sum_{m=1}^{\infty}W_m(x)e^{i\omega t}\sin(\alpha_m y), \tag{13}$$

where $\alpha_m = m\pi/L$; $(m=1,2,\ldots\ldots,\infty)$. This leads to an ordinary differential equation expressed as:

$$\frac{\mathrm{d}^4W_m(x)}{\mathrm{d}x^4}-\left(2\alpha_m^2+\frac{k_p}{D_{\text{sfgm}}}\right)\frac{\mathrm{d}^2W_m(x)}{\mathrm{d}x^2}+\left(\alpha_m^4+\frac{k_w}{D_{\text{sfgm}}}-\frac{\alpha_m^2k_p}{D_{\text{sfgm}}}-\frac{I_0\omega^2}{D_{\text{sfgm}}}\right)W_m(x)=0. \tag{14}$$

Depending on the nature of the roots, two distinct cases are possible:

Case 1.

$$\left(\alpha_m^2+\frac{k_p}{2D_{\text{sfgm}}}\right)\geq\sqrt{\left(\frac{k_p^2}{4D_{\text{sfgm}}^2}+\frac{I_0\omega^2}{D_{\text{sfgm}}}-\frac{k_w}{D_{\text{sfgm}}}\right)} \tag{15}$$

In this case, all the four roots are real $(t_{1m}, -t_{1m}, t_{2m}, -t_{2m})$

$$\begin{aligned} t_{1m} &= \sqrt{\left(\alpha_m^2+\frac{k_p}{2D_{\text{sfgm}}}\right)+\sqrt{\left(\frac{k_p^2}{4D_{\text{sfgm}}^2}+\frac{I_0\omega^2}{D_{\text{sfgm}}}-\frac{k_w}{D_{\text{sfgm}}}\right)}} \\ t_{2m} &= \sqrt{\left(\alpha_m^2+\frac{k_p}{2D_{\text{sfgm}}}\right)-\sqrt{\left(\frac{k_p^2}{4D_{\text{sfgm}}^2}+\frac{I_0\omega^2}{D_{\text{sfgm}}}-\frac{k_w}{D_{\text{sfgm}}}\right)}} \end{aligned} \tag{16}$$

The solution for the case where all the roots are real is expressed as:

$$W_m(x)=A_{1m}\cosh(t_{1m}x)+A_{2m}\sinh(t_{1m}x)+A_{3m}\cosh(t_{2m}x)+A_{4m}\sinh(t_{2m}x) \tag{17}$$

Case 2.

$$\left(\alpha_m^2+\frac{k_p}{2D_{\text{sfgm}}}\right)<\sqrt{\left(\frac{k_p^2}{4D_{\text{sfgm}}^2}+\frac{I_0\omega^2}{D_{\text{sfgm}}}-\frac{k_w}{D_{\text{sfgm}}}\right)} \tag{18}$$

In this case, two real and imaginary roots are possible $(t_{1m}, -t_{1m}, it_{2m}, -it_{2m})$

$$t_{1m} = \sqrt{\left(\alpha_m^2 + \frac{k_p}{2D_{\text{sfgm}}}\right) + \sqrt{\left(\frac{k_p^2}{4D_{\text{sfgm}}^2} + \frac{I_0\omega^2}{D_{\text{sfgm}}} - \frac{k_w}{D_{\text{sfgm}}}\right)}}$$
$$t_{2m} = \sqrt{-\left(\alpha_m^2 + \frac{k_p}{2D_{\text{sfgm}}}\right) + \sqrt{\left(\frac{k_p^2}{4D_{\text{sfgm}}^2} + \frac{I_0\omega^2}{D_{\text{sfgm}}} - \frac{k_w}{D_{\text{sfgm}}}\right)}} \tag{19}$$

The solution for this case is:

$$W_m(x) = A_{1m}\cosh(t_{1m}x) + A_{2m}\sinh(t_{1m}x) + A_{3m}\cos(t_{2m}x) + A_{4m}\sin(t_{2m}x) \tag{20}$$

The dynamic stiffness matrix for case 2 is developed here. The formulation of dynamic stiffness matrix for case 1 follows exactly similar procedure, and it is omitted here. Once the displacement w_0 is known, the expressions for the rotation ϕ_y, shear force V_x, and the bending moment M_{xx} are developed. Rotation:

$$\begin{aligned}\phi_{ym} &= \Phi_{ym}\sin(\alpha_m y)\\ &= -[A_{1m}t_{1m}\sinh(t_{1m}x) + A_{2m}t_{1m}\cosh(t_{1m}x) - A_{3m}t_{2m}\sin(t_{2m}x) + A_{4m}t_{2m}\cos(t_{2m}x)]\end{aligned} \tag{21}$$

Shear force:

$$\begin{aligned}V_x &= -D_{\text{sfgm}}\left(\frac{\mathrm{d}^3W_m}{\mathrm{d}x^2} + (\mu-2)\alpha_m\frac{\mathrm{d}W_m}{\mathrm{d}x}\right) + k_p\frac{\mathrm{d}W_m}{\mathrm{d}x}\\ &= -D_{\text{sfgm}}\left[A_{1m}\left(t_{1m}^3 - (2-\mu)\alpha_m^2t_{1m} + \frac{k_pt_{1m}}{D_{\text{sfgm}}}\right)\sinh(t_{1m}x)\right.\\ &\quad + A_{2m}\left(t_{1m}^3 - (2-\mu)\alpha_m^2t_{1m} + \frac{k_pt_{1m}}{D_{\text{sfgm}}}\right)\cosh(t_{1m}x)\\ &\quad + A_{3m}\left(t_{2m}^3 - (2-\mu)\alpha_m^2t_{2m} + \frac{k_pt_{2m}}{D_{\text{sfgm}}}\right)\sin(t_{2m}x)\\ &\quad \left. - A_{4m}\left(t_{2m}^3 - (2-\mu)\alpha_m^2t_{2m} + \frac{k_pt_{2m}}{D_{\text{sfgm}}}\right)\cos(t_{2m}x)\right]\end{aligned} \tag{22}$$

Bending moment:

$$\begin{aligned}M_{xx_m}(x,y) &= M_{xx_m}\sin(\alpha_m y)\\ &= -D_{\text{sfgm}}\left[A_{1m}(t_{1m}^2 - \mu\alpha_m^2)\cosh(t_{1m}x) + A_{2m}(t_{1m}^2 - \mu\alpha_m^2)\sinh(t_{1m}x)\right.\\ &\quad \left. - A_{3m}(t_{2m}^2 + \mu\alpha_m^2)\cos(t_{2m}x) - A_{4m}(t_{2m}^2 + \mu\alpha_m^2)\sin(t_{2m}x)\right]\end{aligned} \tag{23}$$

Now, the displacement BCs are:

$$\begin{aligned}&\text{At } x = 0: \ W_m = \widetilde{W}_1,\ \Phi_{y_m} = \widetilde{\Phi}_{y_1},\\ &\text{At } x = b: \ W_m = \widetilde{W}_2,\ \Phi_{y_m} = \widetilde{\Phi}_{y_2}.\end{aligned} \tag{24}$$

Similarly, the force BCs:

$$\begin{aligned}&\text{At } x = 0: \ V_{xm} = -\widetilde{V}_1,\ M_{xx_m} = -\widetilde{M}_1,\\ &\text{At } x = b: \ V_{xm} = \widetilde{V}_2,\ M_{xx_m} = \widetilde{M}_2.\end{aligned} \tag{25}$$

Substituting Eq. (24) into Eqs. (20) and (21) yields the following matrix for the displacement components.

$$\begin{bmatrix}\widetilde{W}_1\\ \widetilde{\Phi}_{y_1}\\ \widetilde{\Phi}_{x_1}\\ \widetilde{W}_2\end{bmatrix} = \begin{bmatrix}1 & 0 & 1 & 0\\ 0 & -t_{1m} & 0 & -t_{2m}\\ C_{h_1} & S_{h_1} & C_2 & S_2\\ -t_{1m}S_{h_1} & -t_{1m}C_{h_1} & t_{2m}S_2 & -t_{2m}C_2\end{bmatrix}\begin{bmatrix}A_{1m}\\ A_{2m}\\ A_{3m}\\ A_{4m}\end{bmatrix} \tag{26}$$

i.e.,

$$\boldsymbol{\delta}_{\mathrm{e}} = \mathbf{X}_{\mathrm{e}}\mathbf{A}_{\mathrm{e}}, \tag{27}$$

where $C_{h_1} = \cosh(t_{im}b)$ and $S_{h_1} = \sinh(t_{im}b)$ with $i = 1, 2$. Again, substituting Eq. (25) into Eq. (22) and (23) yields the following matrix relation for the force components.

$$\begin{bmatrix} \widetilde{V}_1 \\ \widetilde{M}_{xx_1} \\ \widetilde{V}_2 \\ \widetilde{M}_{xx_2} \end{bmatrix} = \begin{bmatrix} 0 & -R_1 & 0 & R_2 \\ -L_1 & 0 & L_2 & 0 \\ R_1 S_{h_1} & R_1 C_{h_1} & R_2 S_2 & -R_2 C_2 \\ L_1 C_{h_1} & L_1 S_{h_1} & -L_2 S_2 & -L_2 C_2 \end{bmatrix} \begin{bmatrix} A_{1m} \\ A_{2m} \\ A_{3m} \\ A_{4m} \end{bmatrix} \tag{28}$$

i.e.,

$$\mathbf{F}_{\mathrm{e}} = \mathbf{Y}_{\mathrm{e}}\mathbf{A}_{\mathrm{e}}, \tag{29}$$

where
$R_i = -D_{\mathrm{sfgm}}\left(t_{im}^3 - (2-\mu)\alpha_m^2 t_{im} + \frac{k_p t_{im}}{D_{\mathrm{sfgm}}}\right)$ and $L_i = -D_{\mathrm{sfgm}}(t_{im}^2 - \mu\alpha_m^2)$ with $i = 1, 2$.
Finally, the dynamic stiffness matrix, $\mathbf{K}_{\mathrm{e}}$, for a single-plate element is obtained by combining Eqs. (27) and (29) as

$$\mathbf{F}_{\mathrm{e}} = \mathbf{K}_{\mathrm{e}}\boldsymbol{\delta}_{\mathrm{e}}, \tag{30}$$

where

$$\mathbf{K}_{\mathrm{e}} = \mathbf{Y}_{\mathrm{e}}\mathbf{X}_{\mathrm{e}}^{-1}. \tag{31}$$

In expanded form, one can write

$$\mathbf{K}_{\mathrm{e}} = \begin{bmatrix} \widetilde{K}_{11} & \widetilde{K}_{12} & \widetilde{K}_{13} & \widetilde{K}_{14} \\ & \widetilde{K}_{22} & \widetilde{K}_{23} & \widetilde{K}_{24} \\ \textbf{Sym} & & \widetilde{K}_{33} & \widetilde{K}_{34} \\ & & & \widetilde{K}_{44} \end{bmatrix} = \begin{bmatrix} [\widetilde{K}_{tt}^{\mathrm{e}}]_{(2*2)} & [\widetilde{K}_{ts}^{\mathrm{e}}]_{(2*2)} \\ [\widetilde{K}_{st}^{\mathrm{e}}]_{(2*2)} & [\widetilde{K}_{ss}^{\mathrm{e}}]_{(2*2)} \end{bmatrix}. \tag{32}$$

The explicit expression for each term of Eq. (32) is not mentioned here due to their larger algebraic expressions.

3.5 Development of dynamic stiffness matrix based on FSDT

Taking reference at the physical neutral surface, the kinematic variables for defining motion of the rectangular plate element are expressed according to the first-order shear deformation theory (FSDT) as [35]:

$$\begin{aligned} u &= z_{\mathrm{pns}}\phi_y(x, y, t) = (z - z_0)\phi_y(x, y, t), \\ v &= -z_{\mathrm{pns}}\phi_x(x, y, t) = -(z - z_0)\phi_x(x, y, t), \\ w &= w_0(x, y, t). \end{aligned} \tag{33}$$

Here, u, v, and w denote the displacement components within the FGM plate in the respective direction, and ϕ_x and ϕ_y are the rotations of the transverse normals along $y-$ and $x-$axis, respectively. Now, through the application of the Hamilton's principle, the following three coupled partial differential equations for the transverse motion of the FGM plate are obtained:

$$\begin{aligned} \widehat{A}_s(w_{0,yy} + w_{0,xx} + \phi_{y,x} - \phi_{x,y}) - k_w w_0 + k_p(w_{0,xx} + w_{0,yy}) &= I_0\ddot{w}_0 \\ D_{\mathrm{sfgm}}(\phi_{y,xx} + ((1-\mu)/2)\phi_{y,yy} - ((1+\mu)/2)\phi_{x,xy}) - \widehat{A}_s(w_{0,x} + \phi_y) &= I_2\ddot{\phi}_y \\ D_{\mathrm{sfgm}}((1-\mu)/2)\phi_{x,xx} + \phi_{x,yy} - ((1+\mu)/2)\phi_{y,xy}) + \widehat{A}_s(w_{0,y} - \phi_x) &= I_2\ddot{\phi}_x \end{aligned} \tag{34}$$

The natural boundary conditions are given as:

$$\begin{aligned} Q_x &: \widehat{A}_s(w_{0,x} + \phi_y) + k_p w_{0,x}, \\ M_{xx} &: D_{\mathrm{sfgm}}(\phi_{y,x} - \mu\phi_{x,y}) \\ M_{xy} &: D_{\mathrm{sfgm}}((1-\mu)/2)(\phi_{x,x} - \phi_{y,y}) \end{aligned} \tag{35}$$

The sign conventions used for defining the displacements and forces are shown in Fig. 2. In these equations, D_{sfgm} is the bending stiffness; $\widehat{A_s}$ is the coefficient of extensional stiffness; I_0 and I_2 are the transverse and rotational inertia of the plate. Mathematical expression of the stiffness and inertia terms is provided in Appendix B.

The solution of Eqs. (34) and (35) will be expressed for Levy form of BCs, where two distinct sides of the plate at $y = 0$ and $y = L$ are simply supported (S) and the remaining other two sides at $x = 0$ and $x = b$ can be either clamped (C), simply supported (S), or free (F).

Solutions that automatically satisfy the Levy-type BCs, i.e., the simply supported condition at both $y = 0$ and $y = L$ edges, are expressed as:

$$\begin{aligned} w_0(x, y, t) &= \sum_{m=1}^{\infty} W_m(x) e^{i\omega t} \sin(\alpha_m y), \\ \phi_y(x, y, t) &= \sum_{m=1}^{\infty} \Phi_{y_m}(x) e^{i\omega t} \sin(\alpha_m y), \\ \phi_x(x, y, t) &= \sum_{m=1}^{\infty} \Phi_{x_m}(x) e^{i\omega t} \cos(\alpha_m y), \end{aligned} \tag{36}$$

where ω represents the angular frequency of the plate, and $\alpha_m = \frac{m\pi}{L}$ with $m = 1, 2, 3, 4, ...\infty$.
Three coupled ordinary differential equations are obtained after substituting Eq. (36) into Eq. (34), and they can be expressed in matrix form as shown below:

$$\begin{bmatrix} \widehat{A}_s(\blacktriangle^2 - \alpha_m^2) + I_0\omega^2 - k_w + k_p(\blacktriangle^2 - \alpha^2) & \widehat{A}_s\blacktriangle & \widehat{A}_s\alpha_m \\ -\widehat{A}_s\blacktriangle & D_{\text{sfgm}}\left(\blacktriangle^2 - \left(\frac{(1-\mu)}{2}\right)\alpha_m^2\right) - \widehat{A}_s + I_2\omega^2 & \frac{(1+\mu)}{2} D_{\text{sfgm}}\alpha_m\blacktriangle \\ \widehat{A}_s\alpha_m & -\frac{(1+\mu)}{2} D_{\text{sfgm}}\alpha_m\blacktriangle & D_{\text{sfgm}}\left(\frac{(1-\mu)}{2}\blacktriangle^2 - \alpha_m^2\right) - \widehat{A}_s + I_2\omega^2 \end{bmatrix} \begin{bmatrix} W_m \\ \Phi_{y_m} \\ \Phi_{x_m} \end{bmatrix} = \begin{bmatrix} 0 \\ 0 \\ 0 \end{bmatrix}, \tag{37}$$

where $\blacktriangle = \frac{d}{dx}$ is a differential operator.
The determinant of Eq. (37) leads us to the following differential equation (Eq. (38)):

$$(\blacktriangle^6 + p_1\blacktriangle^4 + p_2\blacktriangle^2 + p_3)\ominus = 0. \tag{38}$$

Here, $\ominus$ represents W_m or Φ_{y_m} or Φ_{x_m}, and p_1, p_2, and p_3 are

$$\begin{aligned} p_1 &= (2\widehat{A_s}^2 - D_{\text{sfgm}}(3\alpha_m^2 k_p + k_w)(-1+\mu) + (I_2 k_p(-3+\mu) + D_{\text{sfgm}} I_0(-1+\mu))\omega^2 \\ &\quad + \widehat{A_s}(-3\alpha_m^2 D_{\text{sfgm}}(-1+\mu) - (-3+\mu)(k_p - I_2\omega^2)))/(D_{\text{sfgm}}(\widehat{A_s} + k_p)(-1+\mu)), \\ p_2 &= (\alpha_m^2 D_{\text{sfgm}}^2(3\alpha_m^2 k_p + 2k_w)(-1+\mu) + D_{\text{sfgm}}(-2\alpha_m^2(I_2 k_p(-3+\mu) + D_{\text{sfgm}} I_0(-1+\mu) \\ &\quad - I_2 k_w(-3+\mu))\omega^2 + I_2(-2I_2 k_p + D_{\text{sfgm}} I_0(-3+\mu))\omega^4 - 2\widehat{A_s}(2\alpha_m^2 D_{\text{sfgm}} + k_p - I_2\omega^2) \\ &\quad + \widehat{A_s}(D_{\text{sfgm}}(2\alpha_m^2 k_p(-3+\mu) + k_w(-3+\mu) + 3\alpha_m^4 D_{\text{sfgm}}(-1+\mu)) + (4I_2 k_p \\ &\quad - D_{\text{sfgm}}(I_0 + 2\alpha_m^2 I_2)(-3+\mu))\omega^2 - 2I_2^2\omega^4)))/(D_{\text{sfgm}}^2(\widehat{A_s} + k_p)(-1+\mu)), \\ p_3 &= (2\widehat{A_s} + \alpha_m^2 D_{\text{sfgm}}(1-\mu) - 2I_2\omega^2)((\alpha_m^2 k_p + k_w - I_0\omega^2)(\alpha_m^2 D_{\text{sfgm}} - I_2\omega^2) \\ &\quad + \widehat{A_s}(\alpha_m^4 D_{\text{sfgm}} + \alpha_m^2 k_p + k_w - (I_0 + \alpha_m^2 I_2)\omega^2)))/(D_{\text{sfgm}}^2(\widehat{A_s} + k_p)(-1+\mu)). \end{aligned} \tag{39}$$

Substituting a trial solution in form of e^{δ} in Eq. (38), the following auxiliary equation is obtained.

$$\delta^6 + p_1\delta^4 + p_2\delta^2 + p_3 = 0. \tag{40}$$

Again, substituting $\eta = \delta^2$ into Eq. (40) reduces it into a cubic polynomial.

$$\eta^3 + p_1\eta^2 + p_2\eta + p_3 = 0. \tag{41}$$

The three roots of Eq. (41) are given by

$$\begin{aligned}
\eta_1 &= -\frac{1}{3}\left(p_1 + \sqrt[3]{\frac{t_1+\sqrt{t_2}}{2}} + \sqrt[3]{\frac{t_1-\sqrt{t_2}}{2}}\right),\\
\eta_2 &= -\frac{1}{3}\left(p_1 + \zeta_2\sqrt[3]{\frac{t_1+\sqrt{t_2}}{2}} + \zeta_1\sqrt[3]{\frac{t_1-\sqrt{t_2}}{2}}\right),\\
\eta_3 &= -\frac{1}{3}\left(p_1 + \zeta_1\sqrt[3]{\frac{t_1+\sqrt{t_2}}{2}} + \zeta_2\sqrt[3]{\frac{t_1-\sqrt{t_2}}{2}}\right),
\end{aligned} \tag{42}$$

with,

$$\begin{aligned}
&\zeta_1 = \frac{i\sqrt{3}-1}{2}, \quad \zeta_2 = -\frac{i\sqrt{3}+1}{2}\\
&t_1 = 2p_1^3 - 9p_1p_2 + 27p_3,\ t_2 = t_1^2 - 4f^3,\ f = p_1^2 - 3p_2.
\end{aligned} \tag{43}$$

Now, the solution of the system of the ordinary differential equations can be written as

$$\begin{aligned}
W_m(x) &= F_1e^{m_1x} + F_2e^{-m_1x} + F_3e^{m_2x} + F_4e^{-m_2x} + F_5e^{m_3x} + F_6e^{-m_3x}\\
\Phi_{y_m}(x) &= G_1e^{m_1x} + G_2e^{-m_1x} + G_3e^{m_2x} + G_4e^{-m_2x} + G_5e^{m_3x} + G_6e^{-m_3x}\\
\Phi_{x_m}(x) &= H_1e^{m_1x} + H_2e^{-m_1x} + H_3e^{m_2x} + H_4e^{-m_2x} + H_5e^{m_3x} + H_6e^{-m_3x}.
\end{aligned} \tag{44}$$

where $m_i = \sqrt{\eta_i}$, and $F_1 - F_6, G_1 - G_6, H_1 - H_6$ are integration constants. These constants are interrelated to each other, and the relation among the constants is found by substituting Eq. (44) into Eq. (37). Simultaneously, solving all the equations and equating each of the term to zero yields the equation in terms of one set of constants, i.e., $(G_1 - G_6)$. The relation between constants is expressed as:

$$\begin{aligned}
F_1 &= \Lambda_1G_1, \quad F_2 = -\Lambda_1G_2, \quad H_1 = \Gamma_1G_1, \quad H_2 = -\Gamma_1G_2,\\
F_3 &= \Lambda_2G_3, \quad F_4 = -\Lambda_2G_4, \quad H_3 = \Gamma_2G_3, \quad H_4 = -\Gamma_2G_4,\\
F_5 &= \Lambda_3G_5, \quad F_6 = -\Lambda_3G_6, \quad H_5 = \Gamma_3G_5, \quad H_6 = -\Gamma_3G_6,
\end{aligned} \tag{45}$$

The extended expressions of Λ_i and Γ_i in terms of material properties are given in Appendix C. Once the relation among the constants (Eq. (45)) is found, the solutions of the system of ordinary differential equation, i.e., Eq. (44), can only be expressed in terms of six integral constants. The solutions in terms of only six integral constant can be expressed as:

$$\begin{aligned}
W_m(x) &= \Lambda_1G_1e^{m_1x} - \Lambda_1G_2e^{-m_1x} + \Lambda_2G_3e^{m_2x} - \Lambda_2G_4e^{-m_2x} + \Lambda_3G_5e^{m_3x} - \Lambda_3G_6e^{-m_3x},\\
\Phi_{y_m}(x) &= G_1e^{m_1x} + G_2e^{-m_1x} + G_3e^{m_2x} + G_4e^{-m_2x} + G_5e^{m_3x} + G_6e^{-m_3x},\\
\Phi_{x_m}(x) &= \Gamma_1G_1e^{m_1x} - \Gamma_1G_2e^{-m_1x} + \Gamma_2G_3e^{m_2x} - \Gamma_2G_4e^{-m_2x} + \Gamma_3G_5e^{m_3x} - \Gamma_3G_6e^{-m_3x},
\end{aligned} \tag{46}$$

Similarly, the expression for forces and moments is found by substituting Eqs. (36) and (46) into Eq. (35). Thus, we get

$$\begin{aligned}
Q_{x_m}(x,y) &= Q_{x_m}(x)\sin(\alpha_m y)\\
&= (\Lambda_1m_1(\widehat{A_s}+k_p) + \widehat{A_s})G_1e^{m_1x} + (\Lambda_1m_1(\widehat{A_s}+k_p) + \widehat{A_s})G_2e^{-m_1x} + (\Lambda_2m_2(\widehat{A_s}+k_p)\\
&\quad + \widehat{A_s})G_3e^{m_2x} + (\Lambda_2m_2(\widehat{A_s}+k_p) + \widehat{A_s})G_4e^{-m_2x} + (\Lambda_3m_3(\widehat{A_s}+k_p) + \widehat{A_s})G_5e^{m_3x}\\
&\quad + (\Lambda_3m_3(\widehat{A_s}+k_p) + \widehat{A_s})G_6e^{-m_3x})\sin(\alpha_m y),\\
M_{xx_m}(x,y) &= M_{xx_m}(x)\sin(\alpha_m y)\\
&= D_{\text{sfgm}}((\mu\alpha_m\Gamma_1 + m_1)G_1e^{m_1x} - (\mu\alpha_m\Gamma_1 + m_1)G_2e^{-m_1x} + (\mu\alpha_m\Gamma_2 + m_2)G_3e^{m_2x}\\
&\quad - (\mu\alpha_m\Gamma_2 + m_2)G_4e^{-m_2x} + (\mu\alpha_m\Gamma_3 + m_3)G_5e^{m_3x} - (\mu\alpha_m\Gamma_3 + m_3)G_6e^{-m_3x})\sin(\alpha_m y),\\
M_{xy_m}(x,y) &= M_{xy_m}(x)\cos(\alpha_m y)\\
&= D_{\text{sfgm}}((1-\mu)/2)((\Gamma_1m_1 - \alpha_m)G_1e^{m_1x} + (\Gamma_1m_1 - \alpha_m)G_2e^{-m_1x} + (\Gamma_2m_2 - \alpha_m)G_3e^{m_2x}\\
&\quad + (\Gamma_2m_2 - \alpha_m)G_4e^{-m_2x} + (\Gamma_3m_3 - \alpha_m)G_5e^{m_3x} + (\Gamma_3m_3 - \alpha_m)G_6e^{-m_3x})\cos(\alpha_m y).
\end{aligned} \tag{47}$$

Once the expression for displacements and forces is obtained, general BCs in terms of algebraic form are used, which can be formulated as:

$$\begin{aligned} &\text{At } x = 0: \; W_m = \widetilde{W}_1, \Phi_{y_m} = \widetilde{\Phi}_{y_1}, \Phi_{x_m} = \widetilde{\Phi}_{x_1} \\ &\text{At } x = b: \; W_m = \widetilde{W}_2, \Phi_{y_m} = \widetilde{\Phi}_{y_2}, \Phi_{x_m} = \widetilde{\Phi}_{x_2} \end{aligned} \tag{48}$$

$$\begin{aligned} &\text{At } x = 0: \; Q_{x_m} = -\widetilde{Q}_1, \; M_{xx_m} = -\widetilde{M}_{xx_1}, \; M_{xy_m} = -\widetilde{M}_{xy_1} \\ &\text{At } x = b: \; Q_{x_m} = \widetilde{Q}_2, \; M_{xx_m} = \widetilde{M}_{xx_2}, \; M_{xy_m} = \widetilde{M}_{xy_2} \end{aligned} \tag{49}$$

The sign convention used for denoting displacements and force components is shown in Fig. 2. By applying BCs for displacements (i.e., substitution of Eq. (48) into Eq. (46)), the following matrix relation is obtained:

$$\begin{bmatrix} \widetilde{W}_1 \\ \widetilde{\Phi}_{y_1} \\ \widetilde{\Phi}_{x_1} \\ \widetilde{W}_2 \\ \widetilde{\Phi}_{y_2} \\ \widetilde{\Phi}_{x_2} \end{bmatrix} = \begin{bmatrix} \Lambda_1 & -\Lambda_1 & \Lambda_2 & -\Lambda_2 & \Lambda_3 & -\Lambda_3 \\ 1 & 1 & 1 & 1 & 1 & 1 \\ \Gamma_1 & -\Gamma_1 & \Gamma_2 & -\Gamma_2 & \Gamma_3 & -\Gamma_3 \\ \Lambda_1 e^{m_1 b} & -\Lambda_1 e^{-m_1 b} & \Lambda_2 e^{m_2 b} & -\Lambda_2 e^{-m_2 b} & \Lambda_3 e^{m_3 b} & -\Lambda_3 e^{-m_3 b} \\ e^{m_1 b} & e^{-m_1 b} & e^{m_2 b} & e^{-m_2 b} & e^{m_3 b} & e^{-m_3 b} \\ \Gamma_1 e^{m_1 b} & -\Gamma_1 e^{-m_1 b} & \Gamma_2 e^{m_2 b} & -\Gamma_2 e^{-m_2 b} & \Gamma_3 e^{m_3 b} & -\Gamma_3 e^{-m_3 b} \end{bmatrix} \begin{bmatrix} G_1 \\ G_2 \\ G_3 \\ G_4 \\ G_5 \\ G_6 \end{bmatrix} \tag{50}$$

i.e.,

$$\boldsymbol{\delta}_{\mathrm{e}} = \mathbf{X}_{\mathrm{e}} \mathbf{G}_{\mathrm{e}}. \tag{51}$$

By applying the force and moment BCs, (i.e., substitution of Eq. (49) into Eq. (47)), the following relationship is obtained:

$$\begin{bmatrix} \widetilde{Q}_{x_1} \\ \widetilde{M}_{xx_1} \\ \widetilde{M}_{xy_1} \\ \widetilde{Q}_{x_2} \\ \widetilde{M}_{xx_2} \\ \widetilde{M}_{xy_2} \end{bmatrix} = \begin{bmatrix} -X_1 & -X_1 & -X_2 & -X_2 & -X_3 & -X_3 \\ -Y_1 & Y_1 & -Y_2 & Y_2 & -Y_3 & Y_3 \\ -Z_1 & -Z_1 & -Z_2 & -Z_2 & -Z_3 & -Z_3 \\ X_1 e^{m_1 b} & X_1 e^{-m_1 b} & X_2 e^{m_2 b} & X_2 e^{-m_2 b} & X_3 e^{m_3 b} & X_3 e^{-m_3 b} \\ Y_1 e^{m_1 b} & -Y_1 e^{-m_1 b} & Y_2 e^{m_2 b} & -Y_2 e^{-m_2 b} & Y_3 e^{m_3 b} & -Y_3 e^{-m_3 b} \\ Z_1 e^{m_1 b} & Z_1 e^{-m_1 b} & Z_2 e^{m_2 b} & Z_2 e^{-m_2 b} & Z_3 e^{m_3 b} & Z_3 e^{-m_3 b} \end{bmatrix} \begin{bmatrix} G_1 \\ G_2 \\ G_3 \\ G_4 \\ G_5 \\ G_6 \end{bmatrix} \tag{52}$$

i.e.,

$$\mathbf{F}_{\mathrm{e}} = \mathbf{Y}_{\mathrm{e}} \mathbf{G}_{\mathrm{e}}, \tag{53}$$

where $X_i = (\Lambda_i m_i (\widehat{A_s} + k_p) + \widehat{A_s})$, $Y_i = D_{\mathrm{sfgm}}(\alpha_m \mu \Gamma_i + m_i)$, $Z_i = D_{\mathrm{sfgm}}((1-\mu)/2)(\Gamma_i m_i - \alpha_m)$, with $i = 1, 2, 3$.

Lastly, the dynamic stiffness matrix, denoted by $\mathbf{K}_{\mathrm{e}}$, for a single FGM plate element is derived from Eqs. (51) and (53) as

$$\mathbf{F}_{\mathrm{e}} = \mathbf{K}_{\mathrm{e}} \boldsymbol{\delta}_{\mathrm{e}}, \tag{54}$$

where

$$\mathbf{K}_{\mathrm{e}} = \mathbf{Y}_{\mathrm{e}} \mathbf{X}_{\mathrm{e}}^{-1}. \tag{55}$$

In matrix form,

$$\mathbf{K}_{\mathrm{e}} = \begin{bmatrix} \hat{K}^*_{11} & \hat{K}^*_{12} & \hat{K}^*_{13} & \hat{K}^*_{14} & \hat{K}^*_{15} & \hat{K}^*_{16} \\ & \hat{K}^*_{22} & \hat{K}^*_{23} & \hat{K}^*_{24} & \hat{K}^*_{25} & \hat{K}^*_{26} \\ & & \hat{K}^*_{33} & \hat{K}^*_{34} & \hat{K}^*_{35} & \hat{K}^*_{36} \\ & & & \hat{K}^*_{44} & \hat{K}^*_{45} & \hat{K}^*_{46} \\ & \mathbf{Sym} & & & \hat{K}^*_{55} & \hat{K}^*_{56} \\ & & & & & \hat{K}^*_{66} \end{bmatrix} = \begin{bmatrix} [\widehat{K^{\mathrm{e}}_{tt}}]_{(3*3)} & [\widehat{K^{\mathrm{e}}_{ts}}]_{(3*3)} \\ [\widehat{K^{\mathrm{e}}_{st}}]_{(3*3)} & [\widehat{K^{\mathrm{e}}_{ss}}]_{(3*3)} \end{bmatrix}. \tag{56}$$

The explicit expression for each term of the symmetric dynamic stiffness matrix, $\mathbf{K_e}$, is not mentioned here due to their larger algebraic expressions.

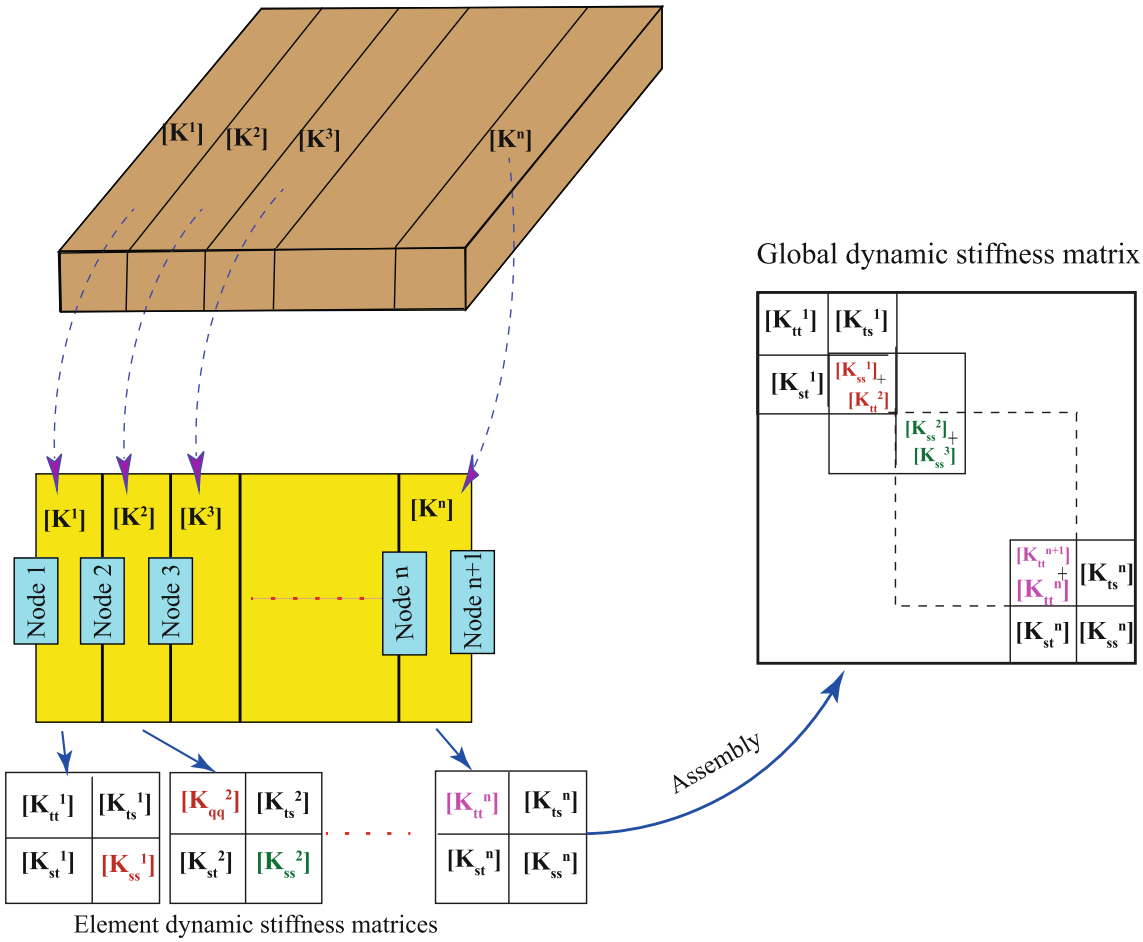

Fig. 3 A pictorial representation of assembly process of DSM

4 Procedure for the computation of modal characteristics of S-FGM plate

It is apparent that the dynamic stiffness matrix derived above is frequency dependent and transcendental in nature. Therefore, an appropriate procedure is to be followed to compute the frequency values accurately. This section briefly discusses the procedure adopted in the present study to compute natural frequencies and mode shapes of the S-FGM plate. Appropriate boundary conditions are enforced on the global dynamic stiffness matrix, which is obtained after assembling individual dynamic stiffness matrix of the plate segment. Thereafter, the Wittrick–Williams (W–W) algorithm is used for the computation of natural frequencies of S-FGM plate.

4.1 Assembly procedure

This section discusses the procedure used in DSM to assemble the individual dynamic stiffness matrix of each plate segment to form a global dynamic stiffness matrix. The assembly procedure used in DSM is quite similar to that of the assembly procedure used in FEM. In the place of point nodes in FEM, line nodes are used in DSM. A pictorial depiction of the assembly procedure of DSM is presented in Fig. 3.

It should be noted that DSM results are generally mesh independent, which means that even with a single element for uniform geometry a convergent result can be obtained. In the case of non-uniform geometry, however, very few elements are required to obtain convergent results which reduces the computational cost significantly.

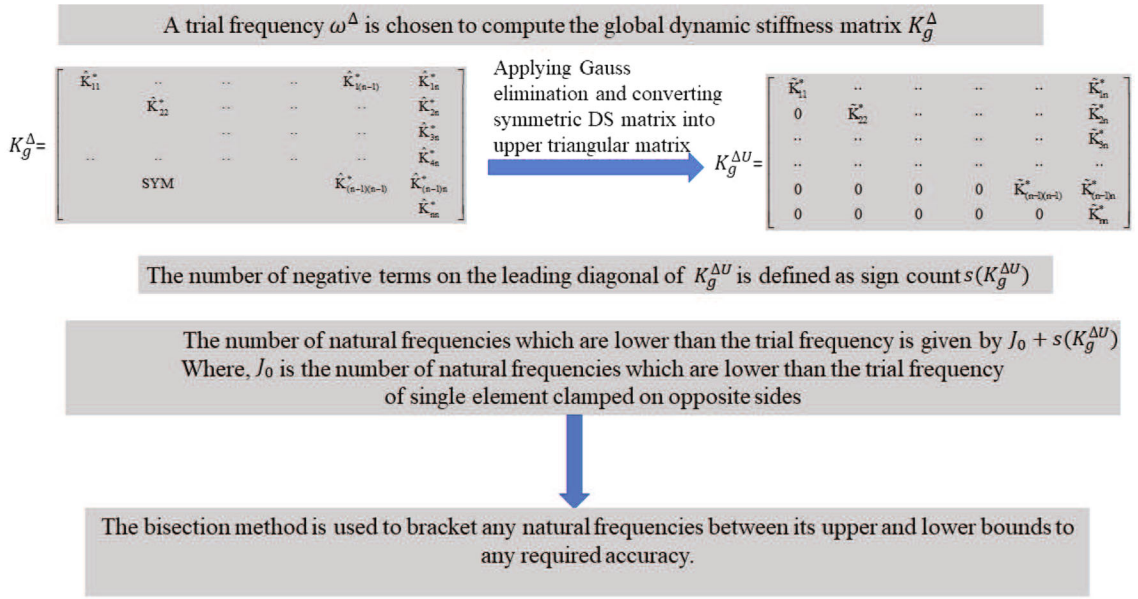

Fig. 4 Wittrick–Williams algorithm for the computation of the natural frequency

4.2 Application of Levy-type boundary conditions

In Levy form of BCs, two distinct sides of the FGM plate, at $y = 0$ and $y = L$, are simply supported, whereas two remaining sides of the plate, at $x = 0$ and $x = b$, can be either clamped (**C**) or simply supported (**S**) or free (**F**). In this study, the penalty method is used to apply these Levy-type boundary constraints. The penalty method allocates a large stiffness to the appropriate term of the leading diagonal of the global dynamic stiffness matrix for the purpose of neutralizing the specific degree of freedom. To be specific, following three cases are considered here.

- For 'Free (F)' edge: No variable needs to be penalized.
- For 'Simply supported (S)' edge: For CPT, W_* is penalized; for FSDT, W_* and Φ_{x*} are penalized.
- For 'Clamped (C)' edge: For CPT, W_*, and Φ_{y_*} are penalized; for FSDT, W_*, Φ_{y_*}, and Φ_{x*} are penalized.

Here, the letter '$*$' signifies the line node on which the appropriate penalty is to be enforced in order to apply the required boundary constraints.

4.3 Procedure to compute natural frequencies and mode shapes

The assembled global dynamic stiffness matrix is transcendental in nature which leads to the transcendental eigenvalue problem. The well-known Wittrick–Williams algorithm [37,38] is used to solve such a transcendental eigenvalue problem. The W–W algorithm ensures that no natural frequency, even the coincident one, is missed in a given frequency range. The procedure for the implementation of W–W algorithm and the development of modeshape is described in many previously published literature [35,36]. Just for the sake of completeness, W–W algorithm is summarized in Fig. 4.

5 Results and discussion

In this section, the natural frequency results for the S-FGM plate resting on elastic foundation for various plate geometries and stiffness parameters are discussed. First, the natural frequencies obtained using DSM based on both CPT and FSDT are validated with the published results. In the subsequent section, the discrepancies in the obtained results and the published results [18] are highlighted. The possible reasons for the mismatch in these results are also discussed. Thereafter, various inferences are made for the free vibration behavior of plates using line diagrams and modeshapes plots.

Table 1 The material property description of S-FGM plate, adopted from [18]

Material constituents Constituents	Material density (kg/m^3)	Young's modulus (GPa)	Poisson's ratio μ
Alumina: Al_2O_3	$\rho_c = 3800$	$E_c = 380$	0.3
Aluminum: Al	$\rho_m = 2707$	$E_m = 70$	0.3

For better understanding of the results, the following two non-dimensional forms for the natural frequency parameters are used in this study: $\bar{\omega} = \omega h\sqrt{\rho_m/E_m}, \hat{\omega} = \omega b^2\sqrt{(\rho_c h/D_c)}$ with $D_c = E_c h^3/(12(1-\mu^2))$. And, the non-dimensional form for the elastic foundation parameters is used as: $K_w = k_w b^4/D_c$ and $K_p = k_p b^2/D_c$. The material properties considered for the constituents of S-FGM plate are mentioned in Table 1.

5.1 Comparison with the published results

In this subsection, the natural frequencies results are compared with that of existing literature wherever possible. Table 2 shows the comparison of the natural frequency results of the S-FGM plate obtained using DSM to that of the results mentioned in Kumar and Jana [14]. Kumar and Jana [14] studied the free vibration behavior of the S-FGM plate using a CPT-based DSM approach. It can be seen that the CPT-based DSM computed results agree perfectly with the published results. Table 2 also contains the natural frequency results of the S-FGM plate using FSDT-based DSM. It is noted that the natural frequency results obtained using DSM based on kinematic variables of FSDT are lesser as compared to that of CPT-based DSM results. This is because FSDT includes the effect of the transverse shear deformation on the vibration of the plate, whereas CPT neglects the transverse shear effect.

For the validation of present analysis results, particularly for the case of plate resting on elastic foundation, the results reported in Baferani et al. [26] have been considered. In that reference the results are reported for FGM plate with power-law (P-FGM) material model. For comparison purposes, we also consider the same material model as given in [26] and the comparison is shown in Table 3. It can be noted that Baferani et al. [26] obtained the accurate natural frequency values of the P-FGM plate resting on Winkler–Pasternak foundation using third-order shear deformation theory. In Table 3, the DSM computed natural frequency results of the square P-FGM plate resting on elastic foundation are compared, with that available in [26], for varying plate thickness ratio (h/b), and varying elastic foundation parameters. It can be seen that the FSDT-based DSM results and the published results are in very good agreement.

Table 4 presents a comparison between the dimensionless fundamental frequency of a SSSS S-FGM plate placed on an elastic foundation and the corresponding values reported in the work of Jung et al. [27]. The comparison considers different coefficients of the elastic foundation (i.e., K_w and K_p) and volume fractions (p) of material components. The fundamental frequencies of the S-FGM plates are evaluated using DSM based on CPT and FSDT. It can be seen that the results obtained using DSM are in good agreement with the published result. As expected, it can been observed that the present CPT and FSDT-based DSM results are higher than that of the results reported in Jung et al. [27] which are based on higher-order shear deformation theory (HSDT).

The above three comparative studies establish that the present method has the capability to compute the natural frequency results very accurately for the FGM plates resting on Winkler–Pasternak foundation. We now proceed to highlight some incorrect results in a recently published paper and discuss the possible reasons for this incorrectness.

5.2 Comments on incorrectly published results

It is emphasized here that Chauhan et al. [18] have attempted to present a CPT-based DSM formulation for the natural frequency computation of S-FGM plate resting on the elastic foundation. However, a careful study can reveal that the mathematical formulation presented in [18], particularly for the elastic foundation cases, is inappropriate. For this reason, most of the results especially those related to the elastic foundation cases are incorrect. Hence, an attempt has been made to present the correct results through the present DSM formulation based on both CPT and FSDT. The results are reported in Table 5. From Table 5, it can be observed that the

Table 2 Validation study of the non-dimensional natural frequency ($\hat{\omega} = \omega b^2\sqrt{(\rho_c h/D_c)}$) with ($D_c = E_c h^3/(12(1-\mu^2))$) of the S-FGM plate with published result for all six BCs [14]. ($b = L,\ h = 0.05b$)

m	n	$p=0$			$p=0.5$			$p=1$			$p=2$			$p=10$		
		Present CPT	Present FSDT	References [14]	Present CPT	Present FSDT	References[14]	Present CPT	Present FSDT	References[14]	Present CPT	Present FSDT	References[14]	Present CPT	Present FSDT	References[14]
SCSC																
1	1	24.0756	23.5436	24.0756	23.1237	22.6451	23.1237	22.0894	21.6645	22.0894	20.8894	20.5214	20.8894	19.4816	19.1735	19.4816
2	1	45.5245	44.1476	45.5245	43.7245	42.4743	43.7245	41.7688	40.6468	41.7688	39.4996	38.5146	39.4996	36.8377	35.9978	36.8377
1	2	57.6525	55.0972	57.6525	55.3731	53.0643	55.3731	52.8963	50.8367	52.8963	50.0226	48.2285	50.0226	46.6515	45.1376	46.6515
2	2	78.6574	74.4738	78.6574	75.5474	71.7490	75.5474	72.1683	68.7607	72.1683	68.2476	65.2582	68.2476	63.6482	61.1029	63.6482
3	1	85.0033	81.0082	85.0033	81.6424	77.9960	81.6424	77.9907	74.6984	77.9907	73.7537	65.2582	73.7537	68.7832	66.2753	68.7832
SCSS																
1	1	19.6643	19.3811	19.6643	18.8869	18.6307	18.8869	18.0421	17.8132	18.0421	17.0619	16.8621	17.0619	15.9121	15.7429	15.9121
2	1	42.9725	41.8880	42.9725	41.2734	40.2860	41.2734	39.4273	38.5381	39.4273	37.2854	36.5012	37.2854	34.7726	34.0998	34.7726
1	2	48.7705	47.1977	48.7705	46.8422	45.4161	46.8422	44.7470	43.4692	44.7470	42.3161	41.1962	42.3161	39.4643	38.5116	39.4643
2	2	71.6296	68.5666	71.6296	68.7976	66.0091	68.7976	65.7204	63.2104	65.7204	62.1500	59.9380	62.1500	57.9615	56.0662	57.9615
3	1	83.3846	79.7041	83.3846	80.0878	76.7256	80.0878	76.5056	73.4667	76.5056	72.3493	69.6568	72.3493	67.4735	65.1502	67.4735
SSSS																
1	1	16.4152	16.2682	16.4152	15.7662	15.6321	15.7662	15.0610	14.9400	15.0610	14.2427	14.1357	14.2427	13.2829	13.1907	13.2829
2	1	41.0379	40.1411	41.0379	39.4154	38.5967	39.4154	37.6524	36.9129	37.6524	35.6069	34.9520	35.6069	33.2072	32.6424	33.2072
1	2	41.0379	40.1411	41.0379	39.4154	38.5967	39.4154	37.6524	36.9129	37.6524	35.6069	34.9520	35.6069	33.2072	32.6424	33.2072
2	2	65.6607	63.4179	65.6607	63.0646	61.0155	63.0646	60.2439	58.3911	60.2439	56.9710	55.3286	56.9710	53.1316	51.7131	53.1316
3	1	82.0759	78.6242	82.0759	78.8308	75.6754	78.8308	75.3048	72.4503	75.3048	71.2137	68.6816	71.2137	66.4145	64.2259	66.4145
SCSF																
1	1	10.5508	10.4321	10.5508	10.1337	10.0250	10.1337	9.6804	9.5820	9.6804	9.1545	9.0672	9.1545	8.5376	8.4622	8.5376
1	2	27.4970	26.7900	27.4970	26.4098	25.7624	26.4098	25.2286	24.6419	25.2286	23.858	23.3370	23.8580	22.2501	21.7998	22.2501
2	1	34.6794	33.9269	34.6794	33.3083	32.6200	33.3083	31.8185	31.1955	31.8185	30.0899	29.5371	30.0899	28.0620	27.5843	28.0620
2	2	52.4033	50.4959	52.4033	50.3314	48.5859	50.3314	48.0802	46.4997	48.0802	45.4681	44.0655	45.4681	42.4039	41.1920	42.4039
1	3	60.2060	57.6785	60.2060	57.8256	55.5117	57.8256	55.2392	53.1430	55.2392	52.2382	50.3764	52.2382	48.7177	47.1068	48.7177
SSSF																
1	1	9.7169	9.6343	9.7169	9.3327	9.2569	9.3327	8.9153	8.8464	8.9153	8.4309	8.3695	8.4309	7.8627	7.8094	7.8627
1	2	23.0822	22.6460	23.0822	22.1696	21.7672	22.1696	21.1780	20.8105	21.1780	20.0275	19.6979	20.0275	18.6778	18.3894	18.6778
2	1	34.2592	33.5540	34.2592	32.9047	32.2594	32.9047	31.4329	30.8486	31.4329	29.7253	29.2064	29.7253	27.7220	27.2731	27.7220
2	2	49.1190	47.6191	49.1190	47.1770	45.8008	47.1770	45.0668	43.8170	45.0668	42.6185	41.5049	42.6185	39.7463	38.7790	39.7463
1	3	51.4434	49.8370	51.4434	49.4095	47.9278	49.4095	47.1995	45.8456	47.1995	44.6353	43.4199	44.6353	41.6272	40.5614	41.6272
SFSF																
1	1	8.0095	7.9631	8.0095	7.6928	7.6503	7.6928	7.3487	7.3102	7.3487	6.9495	6.9153	6.9495	6.4811	6.4516	6.4811
1	2	13.4177	13.1868	13.4177	12.8872	12.6740	12.8872	12.3108	12.1159	12.3108	11.6420	11.4671	11.6420	10.8574	10.7045	10.8574
1	3	30.5411	29.7041	30.5411	29.3336	28.5569	29.3336	28.0216	27.3074	28.0216	26.4992	25.8538	26.4992	24.7134	24.1433	24.7134
2	1	32.3867	31.7700	32.3867	31.1062	30.5423	31.1062	29.7149	29.2046	29.7149	28.1006	27.6478	28.1006	26.2068	25.8154	26.2068
2	2	38.8676	37.8317	38.8676	37.3308	36.3797	37.3308	35.6611	34.7967	35.6611	33.7237	32.9530	33.7237	31.4510	30.7811	31.4510

Table 3 Non-dimensional fundamental frequency ($\bar{\omega} = \omega h\sqrt{\rho_m/E_m}$) comparison of a square P-FGM plate resting on elastic foundation for two different BCs with that of the result given in reference [26]

K_w	K_p	h/b	$p=0$			$p=1$			$p=2$			$p=5$		
			References[26]	Present (FSDT)	Present (CPT)	References[26]	Present (FSDT)	Present (CPT)	References[26]	Present (FSDT)	Present (CPT)	References[26]	Present (FSDT)	Present (CPT)
SSSS														
0	0	0.05	0.0291	0.0291	0.0293	0.0227	0.0222	0.0224	0.0209	0.0202	0.0204	0.0197	0.0191	0.0193
		0.1	0.1134	0.1133	0.1174	0.0891	0.0868	0.0896	0.0819	0.0788	0.0815	0.0767	0.0744	0.0772
		0.15	0.2454	0.2452	0.2641	0.1939	0.1885	0.2016	0.1778	0.1711	0.1833	0.1648	0.1606	0.1738
		0.20	0.4154	0.4150	0.4694	0.3299	0.3205	0.3583	0.3016	0.2905	0.3258	0.2765	0.2711	0.3090
0	100	0.05	0.0406	0.0406	0.0407	0.0382	0.0380	0.0380	0.0380	0.0374	0.0376	0.0381	0.0377	0.0378
		0.10	0.1599	0.1597	0.1632	0.1517	0.1494	0.1518	0.1508	0.1478	0.1502	0.1515	0.1488	0.1513
		0.15	0.3515	0.3512	0.3671	0.3365	0.3304	0.3416	0.3351	0.3272	0.3379	0.3362	0.3293	0.3405
		0.20	0.6080	0.6074	0.6527	0.5876	0.5755	0.6073	0.5861	0.5703	0.6007	0.5879	0.5742	0.6053
100	0	0.05	0.0298	0.0298	0.0300	0.0238	0.0233	0.0234	0.0221	0.0214	0.0216	0.0210	0.0204	0.0210
		0.10	0.1162	0.1161	0.1201	0.0933	0.0910	0.0937	0.0867	0.0837	0.0863	0.0821	0.0798	0.0826
		0.15	0.2519	0.2516	0.2702	0.2036	0.1982	0.2109	0.1889	0.1822	0.1941	0.1775	0.1732	0.1859
		0.20	0.4273	0.4268	0.4804	0.3476	0.3381	0.3749	0.3219	0.3108	0.3451	0.2999	0.2941	0.3304
100	100	0.05	0.0411	0.0410	0.0412	0.0388	0.0384	0.0386	0.0386	0.0381	0.0382	0.0388	0.0384	0.0385
		0.10	0.1619	0.1617	0.1652	0.1542	0.1518	0.1543	0.1535	0.1505	0.1528	0.1543	0.1516	0.1541
		0.15	0.3560	0.3557	0.3716	0.3422	0.3360	0.3472	0.3412	0.3331	0.3439	0.3427	0.3356	0.3468
		0.20	0.6162	0.6156	0.6606	0.5978	0.5854	0.6172	0.5970	0.5809	0.6114	0.5993	0.5853	0.6165
SCSC														
0	0	0.05	0.0421	0.0421	0.0430	0.0324	0.0322	0.0328	0.0295	0.0293	0.0298	0.0278	0.0277	0.0283
		0.10	0.1589	0.1585	0.1721	0.1239	0.1222	0.1314	0.1125	0.1110	0.1195	0.1043	0.1039	0.1133
		0.15	0.3300	0.3284	0.3873	0.2600	0.2554	0.2956	0.2353	0.2316	0.2688	0.2144	0.2148	0.2549
		0.20	0.5363	0.5317	0.6885	0.4263	0.4169	0.5255	0.3844	0.3776	0.4779	0.3447	0.3469	0.4532
0	100	0.05	0.0515	0.0515	0.0523	0.0457	0.0454	0.0459	0.0443	0.0439	0.0445	0.0440	0.0437	0.0443
		0.10	0.1972	0.1967	0.2094	0.1777	0.1753	0.1839	0.1729	0.1703	0.1782	0.1705	0.1686	0.1772
		0.15	0.4195	0.4174	0.4711	0.3846	0.3775	0.4137	0.3751	0.3675	0.4010	0.3687	0.3635	0.3988
		0.20	0.7033	0.6977	0.4532	0.6556	0.6410	0.7354	0.6421	0.6262	0.7129	0.6308	0.6200	0.7089
100	0	0.05	0.0426	0.0426	0.0435	0.0332	0.0329	0.0336	0.0304	0.0301	0.0307	0.0288	0.0286	0.0293
		0.10	0.1609	0.1605	0.1740	0.1269	0.1252	0.1342	0.1161	0.1145	0.1228	0.1084	0.1079	0.1170
		0.15	0.3349	0.3332	0.3915	0.2673	0.2626	0.3021	0.2438	0.2399	0.2763	0.2243	0.2243	0.2633
		0.20	0.5457	0.5411	0.6960	0.4402	0.4306	0.5370	0.4007	0.3935	0.4912	0.3639	0.3653	0.4681
00	100	0.05	0.0519	0.0518	0.0527	0.0462	0.0458	0.0464	0.0449	0.0446	0.0451	0.0446	0.0443	0.0449
		0.10	0.1988	0.1983	0.2109	0.1799	0.1775	0.1859	0.1752	0.1726	0.1805	0.1730	0.1711	0.1796
		0.15	0.4233	0.4212	0.4746	0.3895	0.3824	0.4183	0.3805	0.3729	0.4061	0.3746	0.3693	0.4042
		0.20	0.7105	0.7049	0.8437	0.6647	0.6500	0.7437	0.6521	0.6360	0.7219	0.6416	0.6305	0.7186

For this comparison, the material properties are adopted from [26]

Table 4 Non-dimensional fundamental frequency ($\bar{\omega} = \omega h\sqrt{\rho_m/E_m}$) comparison of a square S-FGM plate resting on elastic foundation with that of the result given in Jung et al. [27]

K_w	K_p	Source	Theory	$p=1$	$p=2$	$p=5$	$p=10$
0	0	Present (DSM)	CPT	8.9627	8.4757	8.0385	7.9045
		Present (DSM)	FSDT	8.9597	8.4732	8.0362	7.9023
		Ref. [27]	HSDT	8.9549	8.4686	8.0319	7.8981
0	100	Present (DSM)	CPT	15.1897	14.9076	14.6635	14.5904
		Present (DSM)	FSDT	15.1871	14.9052	14.6612	14.5882
		Ref. [27]	HSDT	15.1789	14.8972	14.6533	14.5804
100	0	Present (DSM)	CPT	9.3781	8.9139	8.4992	8.3726
		Present (DSM)	FSDT	9.3752	8.9114	8.4970	8.3704
		Ref. [27]	HSDT	9.3702	8.9066	8.4924	8.3660
100	100	Present (DSM)	CPT	15.4385	15.1610	14.9210	14.8492
		Present (DSM)	FSDT	15.4359	15.1586	14.9187	14.8470
		Ref. [27]	HSDT	15.4276	15.1504	14.9107	14.8390

All the edges of the plate are simply supported. Here, $L = b,\ h = 0.01b,\ K_w = k_w b^4/D_m,\ K_p = k_p b^2/D_m,\ D_m = E_m h^3/(12(1-\mu^2))$

Table 5 Comparative study of non-dimensional fundamental frequency ($\hat{\omega} = \omega b^2\sqrt{(\rho_c h/D_c)}$) with ($D_c = E_c h^3/(12(1-\mu^2))$) of square S-FGM plate resting on elastic foundation with that of the results mentioned in [18]

K_w	K_p	$p=0$				$p=1$				$p=2$				$p=10$			
		Present (CPT)	Present (FSDT)	References [18]	% Err	Present (CPT)	Present (FSDT)	References [18]	% Err	Present (CPT)	Present (FSDT)	References [18]	% Err	Present (CPT)	Present (FSDT)	References [18]	% Err
SCSC																	
0	0	24.0756	24.0533	24.0576	0.0	22.0894	22.0717	22.0894	0.0	20.8894	20.8741	20.8893	0.0	19.4816	19.4688	19.4815	0.0
100	0	26.3900	26.3692	25.4713	3.4	24.5915	24.5751	23.3700	4.9	23.5194	23.5053	22.1004	6.0	22.2784	22.2667	20.6110	7.4
0	100	55.4421	55.4148	45.4730	17.9	54.5447	54.5210	41.7216	23.5	54.0264	54.0046	39.4550	26.9	53.4417	53.4219	36.7960	31.1
100	100	56.4856	56.4586	46.2272	18.1	55.6051	55.5816	42.4135	23.7	55.0967	55.0751	40.1093	27.2	54.5236	54.5039	37.4062	31.3
SCSS																	
0	0	19.6643	19.6526	19.6643	0.0	18.0421	18.0327	18.0420	0.0	17.0619	17.0537	17.0619	0	15.9121	15.9051	15.9120	0.0
100	0	22.4384	22.4277	21.3504	4.8	21.0313	21.0227	19.5891	6.8	20.1967	20.1892	18.5248	8.2	19.2351	19.2288	17.2764	10.1
0	100	52.8830	52.8685	42.6788	19.2	52.2574	52.2443	39.1579	25.0	51.8980	51.8856	37.0306	28.6	51.4945	51.4830	34.5350	32.9
100	100	53.9760	53.9616	43.4814	19.4	53.3632	53.3501	39.8943	25.2	53.0113	52.9990	37.727	28.8	52.6164	52.6048	35.1845	33.1
SSSS																	
0	0	16.4152	16.4092	16.4151	0.0	15.061	15.0561	15.0609	0.0	14.2427	14.2384	14.2427	0.0	13.2829	13.2792	13.2828	0.0
100	0	19.6534	19.6479	18.4014	6.3	18.5373	18.5327	16.8834	8.9	17.8788	17.8748	15.9661	10.6	17.1240	17.1205	14.8901	13.0
0	100	50.7439	50.7382	40.4295	20.3	50.3222	50.3166	37.0942	26.2	50.0834	50.0779	35.0789	29.9	49.8189	49.8134	32.7149	34.3
100	100	51.8820	51.8763	41.2759	20.4	51.4696	51.4639	37.8707	26.4	51.2361	51.2305	35.8133	30.1	50.9776	50.9721	33.3998	34.4
SCSF																	
0	0	10.5508	10.5385	10.5508	0.0	9.6804	9.6701	9.6804	0.0	9.1545	9.1453	9.1545	0.0	8.5376	8.5296	8.5375	0.0
100	0	15.1036	15.0945	13.4341	11.0	14.5089	14.5015	12.3258	15.0	14.1634	14.1569	11.6562	17.7	13.7727	13.7672	10.8706	21.0
0	100	39.9458	39.9406	42.8405	−7.2	39.6811	39.6763	39.3063	0.9	39.5294	39.5248	37.1709	5.9	39.3595	39.3551	34.6658	11.9
100	100	41.3819	41.3768	43.6402	−5.4	41.1265	41.1217	40.0400	2.6	40.9802	40.9756	37.8647	7.6	40.8163	40.8119	35.3129	13.4
SSSF																	
0	0	9.7169	9.7084	9.7168	0.0	8.9153	8.9082	8.9152	0.0	8.4309	8.4246	8.4309	0.0	7.8627	7.8572	7.8627	0.0
100	0	14.5332	14.5272	12.7896	11.9	14.0100	14.0050	11.7345	16.2	13.7069	13.7024	11.0970	19.0	13.3649	13.3611	10.3491	22.5
0	100	39.2826	39.2799	40.5462	−3.2	39.0789	39.0763	37.2013	4.8	38.9635	38.9609	35.1802	9.7	38.8357	38.8331	32.8093	15.5
100	100	40.7421	40.7394	41.3903	−1.5	40.5457	40.5430	37.9757	6.3	40.4346	40.4318	35.9126	11.1	40.3114	40.3087	33.4923	16.9
SFSF																	
0	0	8.0095	8.0058	8.0094	0.0	7.3487	7.3456	7.3487	0.0	6.9495	6.9467	6.9494	0.0	6.4811	6.4787	6.4811	0.0
100	0	13.4517	13.4492	11.5459	14.1	13.0691	13.0669	10.5934	18.9	12.8488	12.8469	10.0178	22.0	12.6017	12.6000	9.3427	25.8
0	100	34.9170	34.9153	40.6658	−16.4	34.7670	34.7653	37.3110	−7.3	34.6823	34.6805	35.2840	−1.7	34.5885	34.5867	32.9061	4.8
100	100	36.5513	36.5495	41.5074	−13.5	36.408	36.4062	38.0832	−4.6	36.3271	36.3252	36.0142	0.8	36.2376	36.2357	33.5871	7.3

The material properties and the non-dimensional representation of the natural frequency are kept same as given in reference [18]. ($b = L,\ h = 0.01b$)

difference in the natural frequency results especially for the plate resting on the elastic foundation parameter is very high. In some cases the difference in both the CPT-based results is as high as 34%. It can be pointed out that this inaccuracy is due to the incorrect mathematical formulation presented in that paper and some of these mistakes are highlighted below.

- The term $k_w \frac{\partial^2 w_0}{\partial t^2}$, associated with the Winkler stiffness coefficient, mentioned in Eq. (15) of reference [18] should be $k_w w_0$ as shown in Eq. (11) of the present paper.
- The term $k_p(\frac{\partial^4 w_0}{\partial x^2 \partial t^2} + \frac{\partial^4 w_0}{\partial y^2 \partial t^2})$ associated with the Pasternak stiffness coefficient mentioned in Eq. (15) of reference [18] should be $k_p(\frac{\partial^2 w_0}{\partial x^2} + \frac{\partial^2 w_0}{\partial y^2})$ as shown in Eq. (11) of the present paper.
- One term associated with the elastic coefficient is missing from the natural BCs equation given in Eq. (16) of reference [18]. The correct expressions are given in Eq. (12) of this paper.
- For Levy-type plate, the reduced governing differential equation i.e., Eq. (18) of Ref. [18] is also incorrect. The correct form of the equation is shown in Eq. (14) of the present paper.
- Furthermore, the important inertia term is missing from the rest of the formulation (i.e., from Eq. (19) to (21)) in reference [18]. The correct mathematical expressions are provided in Sect. 3.4 of this paper.

Note that the above mistakes may not be treated as typographical errors as similar mistakes have been found in another recent paper [42] published by the same group of authors. Therefore, in this study, these mistakes in the CPT-based DSM formulation presented in reference [18] have been identified and the correct formulation is presented. For the frequency analysis of S-FGM plate, correct results are obtained using both CPT- and FSDT-based DSM formulation. Importantly, the present DSM results are validated with the available literature and they are found to be in good agreement with that of the published results.

5.3 Parametric study

This section discusses the frequency results for S-FGM plates by changing the plate geometry and stiffness parameters of the elastic foundation. Frequency results for the square S-FGM plates can be found in Table 5 for all six Levy type BCs, whereas Tables 6 and 7 show the natural frequency results of the S-FGM plate resting on elastic foundation for two different aspect ratios i.e., $L/b = 0.5$ and $L/b = 2$, respectively. The natural frequency results are shown for varying volume fractions of the material constituents. It can be seen that the natural frequency for the plate with higher aspect ratio ($L/b = 2$) is lesser as compared to that of the plate with smaller aspect ratio ($L/b = 0.5$) as we keep all other parameters same. The reason for this behavior is that the plate with larger dimensions offers lesser bending stiffness as compared to that of the plate with smaller dimensions. One noteworthy point is that the natural frequency results for the DSM based on FSDT are lesser as compared to the result obtained using DSM based on CPT. This trend is as per expectation as FSDT-based formulation considers the shear deformation of the plate, whereas CPT ignores the shear effect.

The effect of elastic foundation on the modeshape of the S-FGM plate can be seen from Fig. 5. Here, the modeshape for the SFSF BCs of the S-FGM plate is shown for the varying coefficients of elastic foundation. From the modeshape plots, it can be seen that the plate with shear foundation offers more bending stiffness as compared to the Winkler foundation.

Figure 6 shows the plot of non-dimensional fundamental frequency with varying volume fraction of the material constituents of S-FGM plate for different elastic modulus parameters and BCs. Figure 6a shows the variation of fundamental frequency with volume fraction p of SSSS S-FGM plate for different elastic modulus coefficients. It can be seen that as the volume fraction increases, the fundamental frequency of the plate decreases. This is due to the increase in metal constituents in the plate as the volume fraction increases. Presence of higher metallic constituents leads lower bending stiffness due to its lower value of the Young's modulus in comparison with that of the ceramic constituent. Figure 6b shows the plot of non-dimensional fundamental frequency for different Levy-type BCs with volume fraction for a plate resting on elastic foundation. It is also observed that the SCSC plate has the highest fundamental frequency and SFSF plate has the lowest.

Figure 7 shows the effect of elastic modulus on the fundamental frequency of a S-FGM plate for varying aspect ratios. Figure 7a shows the variation for the S-FGM plate resting on Winkler foundation, whereas Fig. 7b shows the variation for S-FGM plate resting on Pasternak foundation. It can be observed that the fundamental frequency of the S-FGM plate decreases as the size of the plate increases and this behavior is expected. We know that plate with smaller sizes provides more resistance to bending as compared to that of plate with larger dimensions. Comparison of Fig. 7a and b also shows that the influence of Pasternak foundation on the natural

Table 6 The non-dimensional fundamental frequency ($\hat{\omega} = \omega b^2\sqrt{(\rho_c h/D_c)}$ with ($D_c = E_c h^3/(12(1-\mu^2))$) of S-FGM rectangular plate ($L/b = 0.5,\ \ h = 0.05b$) resting on elastic foundation for different BCs and varying volume fractions (n) of the material constituents

K_w	K_p	$p = 0$		$p = 0.5$		$p = 1$		$p = 2$		$p = 10$	
		Present (CPT)	Present (FSDT)	Present (CPT)	Present (FSDT)	Present (CPT)	Present (FSDT)	Present (CPT)	Present) (FSDT)	Present (CPT)	Present (FSDT)
SCSC											
0	0	45.5245	44.1476	43.7245	42.4743	41.7688	40.6468	39.4996	38.5146	36.8377	35.9978
100	0	46.7897	45.4388	45.0403	43.8142	43.1443	42.0443	40.9514	39.9859	38.3902	37.5669
0	100	89.4210	88.1960	88.5060	87.3556	87.5419	86.4649	86.4638	85.4623	85.2562	84.3312
100	100	90.0717	88.8494	89.1634	88.0150	88.2065	87.1307	87.1366	86.1355	85.9384	85.0129
SSSC											
0	0	42.9725	41.8880	41.2734	40.2860	39.4273	38.5381	37.2854	36.5012	34.7726	34.0998
100	0	44.3106	43.2467	42.6649	41.6963	40.8817	40.0095	38.8200	38.0505	36.4133	35.7525
0	100	87.7223	86.7753	86.8952	85.9972	86.025	85.1745	85.0536	84.2511	83.9681	83.2131
100	100	88.3855	87.4393	87.5647	86.6669	86.7012	85.8503	85.7375	84.9339	84.6607	83.9040
SSSS											
0	0	41.0379	40.1411	39.4154	38.5967	37.6524	36.9129	35.6069	34.9520	33.2072	32.6424
100	0	42.4371	41.5571	40.8702	40.0667	39.1727	38.4467	37.2108	36.5673	34.9216	34.3655
0	100	86.3008	85.5579	85.5411	84.8298	84.7433	84.0617	83.8544	83.2020	82.8640	82.2390
100	100	86.9749	86.2313	86.2211	85.5087	85.4296	84.7464	84.5480	83.8934	83.5657	82.9380
SCSF											
0	0	34.6794	33.9269	33.3083	32.6200	31.8185	31.1955	30.0899	29.5371	28.0620	27.5843
100	0	36.3244	35.5928	35.0177	34.3487	33.6038	32.9982	31.9718	31.4343	30.0712	29.6060
0	100	78.4458	77.8437	77.8369	77.2596	77.1973	76.6434	76.4845	75.9538	75.6897	75.1811
100	100	79.1868	78.5842	78.5836	78.0053	77.9501	77.3948	77.2443	76.7117	76.4573	75.9463
SSSF											
0	0	34.2592	33.5540	32.9047	32.2594	31.4329	30.8486	29.7253	29.2064	27.7220	27.2731
100	0	35.9234	35.2376	34.6340	34.0066	33.2389	32.6706	31.6289	31.1239	29.7541	29.3164
0	100	78.0775	77.5254	77.4849	76.9534	76.8629	76.3507	76.1703	75.6770	75.3990	74.9231
100	100	78.8219	78.2689	78.2350	77.7022	77.6189	77.1050	76.9332	76.4376	76.1696	75.6909
SFSF											
0	0	32.3867	31.7700	31.1062	30.5423	29.7149	29.2046	28.1006	27.6478	26.2068	25.8154
100	0	34.1423	33.5442	32.9301	32.3832	31.6192	31.1241	30.1071	29.6674	28.3477	27.9667
0	100	75.3346	74.8427	74.7877	74.3132	74.2140	73.7556	73.5755	73.1328	72.8650	72.4366
100	100	76.1058	75.6130	75.5646	75.0887	74.9967	74.5366	74.3650	73.9200	73.6621	73.2310

Table 7 The non-dimensional fundamental frequency ($\hat{\omega} = \omega b^2\sqrt{(\rho_c h/D_c)}$ with ($D_c = E_c h^3/(12(1-\mu^2))$) of S-FGM rectangular plate ($L/b = 2,\ h = 0.05b$) resting on elastic foundation for different BCs and varying volume fractions (p) of the material constituents

K_w	K_p	$p = 0$		$p = 0.5$		$p = 1$		$p = 2$		$p = 10$	
		Present (CPT)	Present (FSDT)	Present (CPT)	Present (FSDT)	Present (CPT)	Present (FSDT)	Present (CPT)	Present) (FSDT)	Present (CPT)	Present (FSDT)
SCSC											
0	0	19.8051	19.4169	19.0221	18.6741	18.1713	17.8636	17.1841	16.9192	16.026	15.8058
100	0	22.5619	22.2144	21.8778	21.5678	21.1422	20.8697	20.3000	20.0667	19.3295	19.1369
0	100	45.0757	44.5096	44.6961	44.1658	44.2929	43.7991	43.8371	43.3827	43.3191	42.9071
100	100	46.3532	45.7995	45.9841	45.4654	45.5923	45.1090	45.1496	44.7047	44.6468	44.2432
SSSC											
0	0	14.4131	14.2436	13.8433	13.6906	13.2241	13.0884	12.5057	12.3879	11.6629	11.5639
100	0	18.0149	17.8705	17.5623	17.4325	17.0785	16.9632	16.5284	16.4282	15.9003	15.8156
0	100	41.9632	41.6914	41.7403	41.4818	41.5042	41.2593	41.2380	41.0079	40.9365	40.7224
100	100	43.3325	43.0658	43.1167	42.8629	42.8881	42.6474	42.6306	42.4040	42.339	42.1278
SSSS											
0	0	10.2595	10.2017	9.8538	9.8012	9.4131	9.3656	8.9017	8.8597	8.3018	8.2656
100	0	14.9015	14.8519	14.6252	14.5792	14.3319	14.2896	14.0014	13.9628	13.6278	13.5930
0	100	39.3216	39.2603	39.2177	39.1562	39.1093	39.0475	38.9894	38.9271	38.8568	38.7937
100	100	40.7797	40.7170	40.6795	40.6165	40.5750	40.5115	40.4594	40.3953	40.3317	40.2666
SCSF											
0	0	4.7433	4.6988	4.5558	4.5150	4.3520	4.3150	4.1156	4.0827	3.8382	3.8098
100	0	11.8024	11.7777	11.7283	11.7053	11.6506	11.6293	11.5644	11.5448	11.4686	11.4508
0	100	25.3607	25.2746	25.2917	25.2093	25.218	25.1396	25.1344	25.0603	25.0387	24.9695
100	100	27.5674	27.4860	27.5039	27.4259	27.4362	27.3618	27.3593	27.2888	27.2715	27.2054
SSSF											
0	0	3.3544	3.3310	3.2218	3.2002	3.0777	3.058	2.9105	2.8928	2.7144	2.6989
100	0	11.3159	11.3032	11.2773	11.2651	11.2370	11.2253	11.1923	11.1811	11.1429	11.1322
0	100	24.3336	24.3187	24.3093	24.2942	24.2838	24.2686	24.2556	24.2402	24.2244	24.2086
100	100	26.6255	26.6097	26.6033	26.5873	26.5801	26.5638	26.5544	26.5377	26.5258	26.5087
SFSF											
0	0	1.9776	1.9739	1.8995	1.8960	1.8145	1.8114	1.7159	1.7132	1.6003	1.5979
100	0	10.9867	10.9833	10.9729	10.9695	10.9585	10.955	10.9427	10.9391	10.9251	10.9215
0	100	17.0979	17.0932	17.0885	17.0837	17.0788	17.0738	17.068	17.0629	17.0561	17.0508
100	100	20.2271	20.2217	20.2192	20.2136	20.2110	20.2052	20.2019	20.1959	20.1918	20.1856

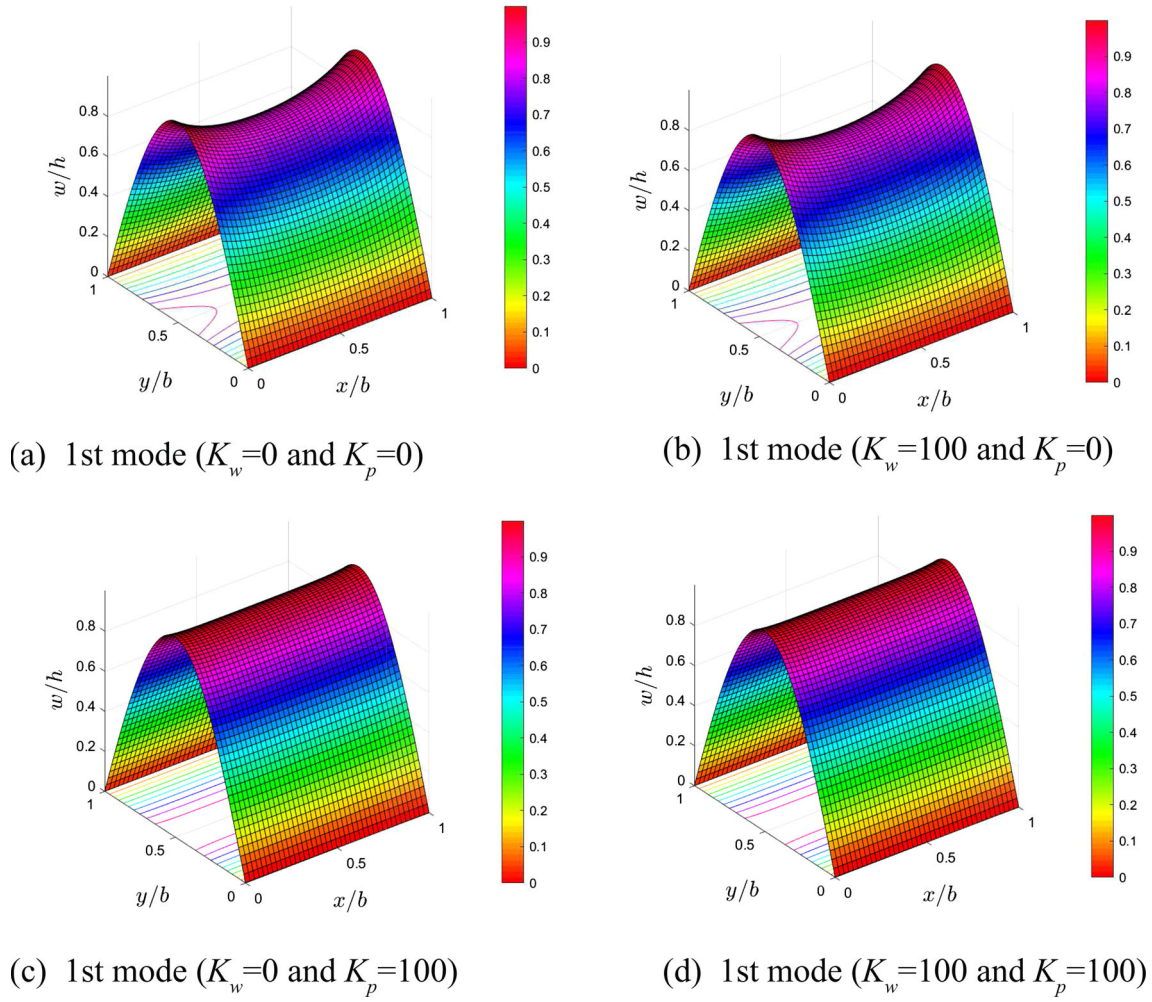

Fig. 5 Modeshapes of the SFSF square plate for varying elastic foundation parameters. ($h = 0.05b,\ p = 2$)

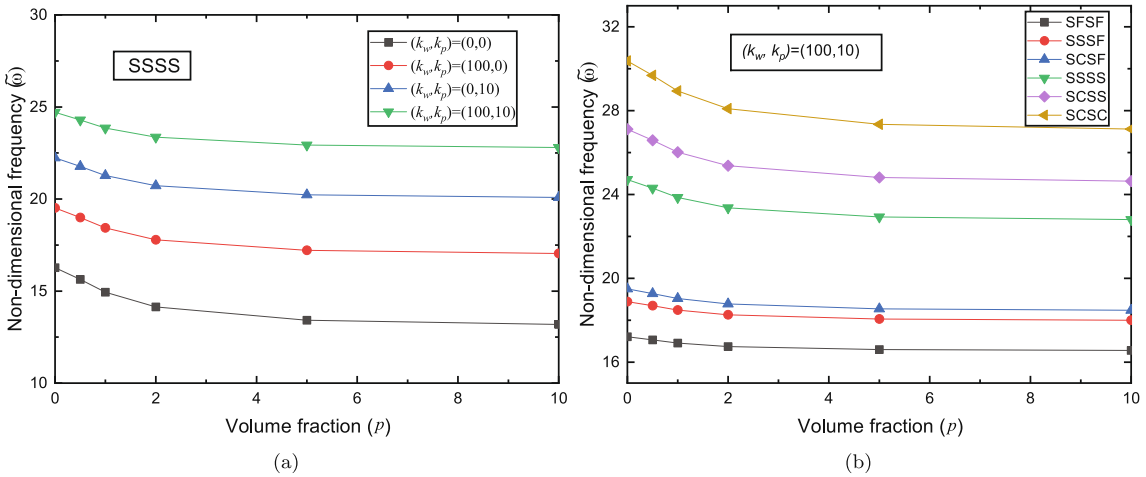

Fig. 6 **a** Plot of non-dimensional fundamental frequency ($\tilde{\omega}$) for different elastic modulus with varying volume fraction of SSSS plate. ($L = b,\ h = 0.05b$). **b** Plot of non-dimensional fundamental frequency ($\tilde{\omega}$) for different boundary conditions with varying volume fraction. For this case, the elastic modulus coefficient is taken as (K_w, K_p) = (100, 10). ($L = b,\ h = 0.05b$)

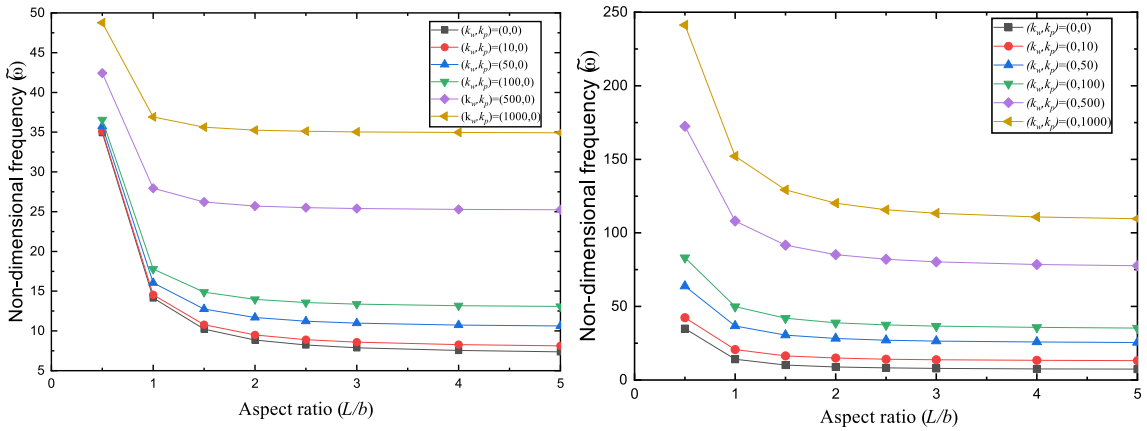

(a) Effect of Winkler elastic foundation (K_w) (b) Effect of Pasternak elastic foundation (K_p)

Fig. 7 Plot of non-dimensional fundamental frequency ($\tilde{\omega}$) for elastic modulus with aspect ratio (L/b). **a** Different Winkler elastic modulus parameter, keeping Pasternak modulus parameter constant vs aspect ratio and **b** different Pasternak elastic modulus parameter keeping, Winkler elastic modulus parameter constant vs aspect ratio. Here, SSSS plate is considered with $h = 0.05b,\ p = 2$

frequency is more as compared to the Winkler foundation. This is due to the fact that the Winkler foundation consists of independent and unconnected springs, whereas the Pasternak foundation has shear layers which exhibits both longitudinal and lateral spring effects leading to higher bending stiffness compared to the Winkler foundation.

Figure 8 shows the modeshapes for different BCs of a S-FGM plate resting on Winkler–Pasternak foundation. It can be noted that, except SFSF plate, there is no visible change in the modeshape for other BCs when one compares the modeshapes of S-FGM plate with and without the Winkler–Pasternak foundation. Modeshapes plots for all these BCs are not shown here for space constraint.

5.4 Comparison study for different plate configurations

It can be emphasized here that the dynamic stiffness method has a potential advantage in the assembly process where dissimilar plate elements can be suitably assemble to study the vibration behavior of plate having non-uniform configurations. To this end, the present section considers two different S-FGM plate configurations as shown in Fig. 9 and present a comparative study of their free vibration characteristics. Table 8 shows the non-dimensional fundamental frequency of stepped plate without elastic foundation shown in Fig. 9a, whereas Table 9 reports the natural frequencies of the plate resting on partial elastic foundation shown in Fig. 9b. These tables show how the fundamental frequencies vary depending on the boundary conditions, thickness ratios, and various elastic foundation coefficients. The frequency results are computed using the dynamic stiffness method and are evaluated using both classical plate theory and the first-order shear deformation theory. The gradual effect of the step thickness on the fundamental frequency of the S-FGM stepped plate can be observed from Table 8, whereas the effect of the Pasternak foundation is quite noticeable as compared to the Winkler foundation in Table 9. The Pasternak foundation offers higher bending stiffness as compared to the Winkler foundation. Additionally, by comparing the data from Tables 8 and 9, it can be inferred that, when all other parameters are held constant, the frequency value for the stepped thickness (h_2/h_1) is more or less comparable to that of the elastic foundation. It can also be observed that to match the frequency of the partially supported S-FGM plate with $K_p = 100$, a sufficiently higher thickness ratio (h_2/h_1) is required. This is because the Pasternak foundation provides a very high bending stiffness due to the presence of shear layer which exhibits both longitudinal and transverse stiffness effects. Nevertheless, the other effects such as the decrease in fundamental frequency as the volume fraction increases, and the fact that SCSC plate has the highest frequency, while SFSF exhibits the lowest frequency, remain unchanged. The reasons behind these patterns align with explanations provided in the previous section.

Figure 10 shows the modal behavior of different configurations of the S-FGM plate. Figure 10a shows the modeshape of the uniform thickness plate without elastic foundation, while Fig. 10b showcases the modeshape

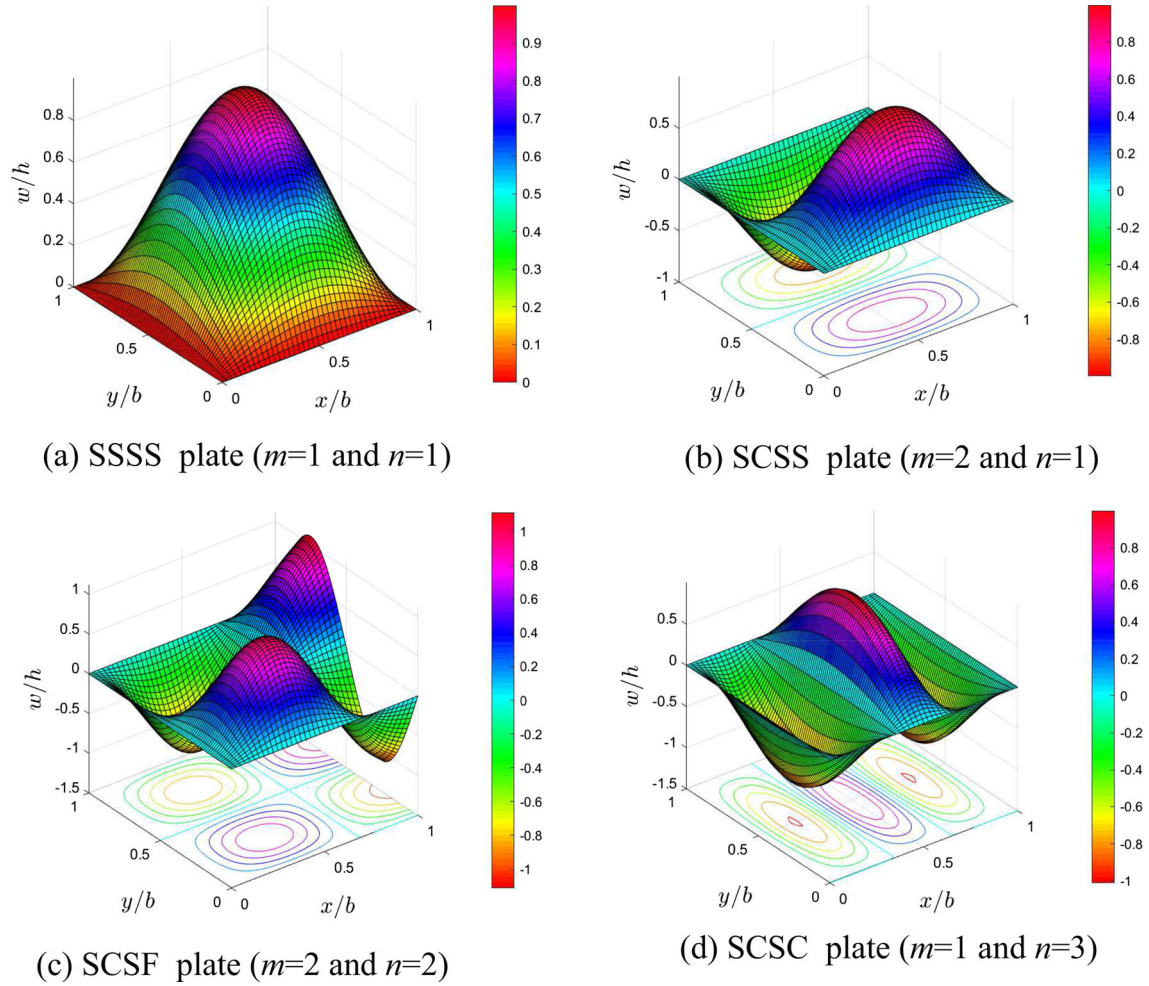

Fig. 8 Mode shape for different BCs of square S-FGM plate resting on Winkler–Pasternak foundation. ($h = 0.05b$, $K_w = 100$, $K_p = 100$)

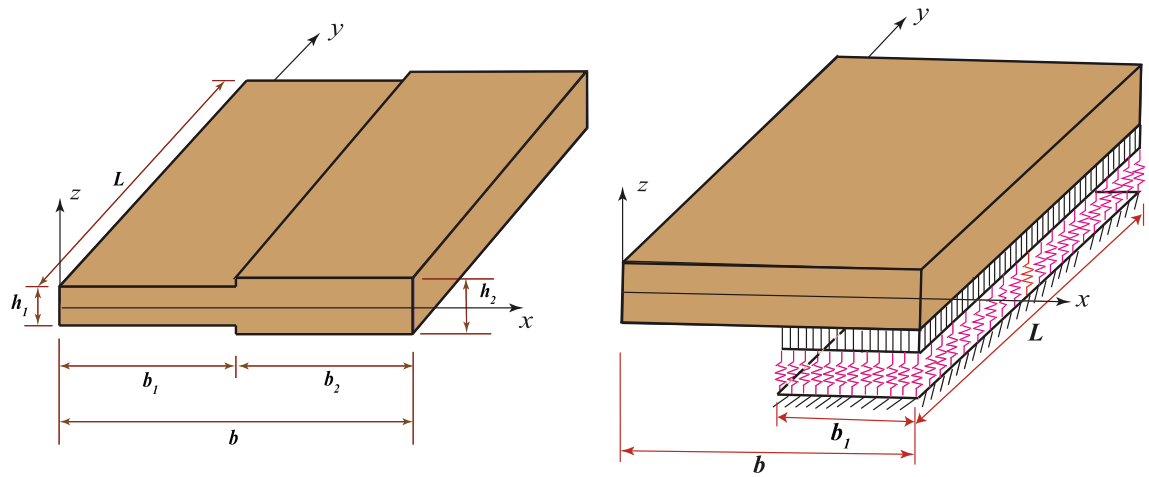

Fig. 9 Two different non-uniform plate configurations considered in this study: **a** stepped plate and **b** plate resting on partial elastic foundation

Table 8 The non-dimensional fundamental frequency ($\hat{\omega} = \omega b^2\sqrt{(\rho_c h/D_c)}$ with ($D_c = E_c h^3/(12(1-\mu^2))$) of S-FGM stepped square plate for different BCs and varying volume fractions (p) of the material constituents. ($L/b = 1,\ \ h = 0.05b,\ \ K_w = K_p = 0$)

h_2/h_1	$p=0$		$p=0.5$		$p=1$		$p=2$		$p=10$	
	CPT	FSDT	CPT	FSDT	CPT	FSDT	CPT	FSDT	CPT	FSDT
SCSC										
1	24.0756	23.5436	23.1237	22.6451	22.0894	21.6645	20.8894	20.5214	19.4816	19.1735
1.5	29.2270	28.2747	28.0714	27.2114	26.8159	26.0491	25.3590	24.6916	23.6500	23.0875
2	34.2349	32.5840	32.8813	31.3806	31.4106	30.0626	29.7041	28.5202	27.7023	26.6932
SCSS										
1	19.6643	19.3811	18.8869	18.6307	18.0421	17.8132	17.0619	16.8621	15.9121	15.7429
1.5	23.9456	23.4462	22.9989	22.5456	21.9702	21.5636	20.7766	20.4198	19.3764	19.0722
2	27.7329	26.8988	26.6364	25.8741	25.445	24.7556	24.0627	23.4517	22.441	21.9138
SSSS										
1	16.4152	16.2682	15.7662	15.6321	15.0610	14.9400	14.2427	14.1357	13.2829	13.1907
1.5	20.0845	19.7960	19.2904	19.0263	18.4275	18.1884	17.4264	17.2139	16.2520	16.0679
2	23.8145	23.2086	22.8729	22.3157	21.8498	21.3424	20.6628	20.2092	19.2703	18.8748
SCSF										
1	10.5508	10.4321	10.1337	10.0250	9.6804	9.5820	9.1545	9.0672	8.5376	8.4622
1.5	14.0124	13.7680	13.4583	13.2348	12.8564	12.6540	12.1579	11.9785	11.3386	11.1837
2	17.3161	16.9283	16.6314	16.2769	15.8875	15.5668	15.0244	14.7401	14.0119	13.7666
SSSF										
1	9.7169	9.6343	9.3327	9.2569	8.9153	8.8464	8.4309	8.3695	7.8627	7.8094
1.5	12.9282	12.7620	12.4170	12.2648	11.8616	11.7236	11.2172	11.0945	10.4613	10.3550
2	16.0902	15.8067	15.454	15.1946	14.7658	14.5279	13.9608	13.7521	13.0199	12.8394
SFSF										
1	8.0095	8.0095	7.6928	7.6503	7.3487	7.3102	6.9495	6.9153	6.4811	6.4516
1.5	10.0673	9.9702	9.6693	9.5803	9.2368	9.1561	8.7350	8.6632	8.1463	8.0842
2	12.2523	12.0337	11.7678	11.5672	11.2415	11.0593	10.6308	10.4686	9.9143	9.7738

Table 9 The non-dimensional fundamental frequency ($\hat{\omega} = \omega b^2\sqrt{(\rho_c h/D_c)}$ with ($D_c = E_c h^3/(12(1-\mu^2))$) of S-FGM square plate resting on partial elastic foundation for different BCs and varying volume fractions (p) of the material constituents. ($L/b = 1,\ \ h = 0.05b,\ \ b_1 = b_2 = 0.5b$)

K_w	K_p	$p = 0$		$p = 0.5$		$p = 1$		$p = 2$		$p = 10$	
		CPT	FSDT	CPT	FSDT	CPT	FSDT	CPT	FSDT	CPT	FSDT
SCSC											
0	0	24.0756	23.5436	23.1237	22.6451	22.0894	21.6645	20.8894	20.5214	19.4816	19.1735
100	0	25.2420	24.7284	24.3342	23.8728	23.3517	22.9425	22.2171	21.8632	20.8948	20.5987
0	100	40.3907	39.6482	39.6468	38.9459	38.8279	38.1683	37.8587	37.2424	36.6854	36.1136
100	100	40.8447	40.0887	40.0933	39.3784	39.2645	38.5906	38.2813	37.6502	37.0875	36.5006
SCSS											
0	0	19.6643	19.3811	18.8869	18.6307	18.0421	17.8132	17.0619	16.8621	15.9121	15.7429
100	0	21.4421	21.1631	20.7291	20.4763	19.9595	19.7330	19.0739	18.8753	18.0463	17.8769
0	100	38.9614	38.4163	38.3428	37.8189	37.6555	37.1526	36.8330	36.3515	35.8231	35.3632
100	100	39.5099	38.9420	38.8795	38.3329	38.1775	37.6519	37.3350	36.8311	36.2971	35.8151
SSSS											
0	0	16.4152	16.2682	15.7662	15.6321	15.0610	14.9400	14.2427	14.1357	13.2829	13.1907
100	0	18.0582	17.9163	17.4661	17.3363	16.8269	16.7092	16.0910	15.9861	15.2366	15.1451
0	100	32.6053	32.2677	32.0011	31.6682	31.3221	30.9936	30.4993	30.1753	29.4762	29.1571
100	100	32.9740	32.6216	32.3549	32.0074	31.6582	31.3156	30.8131	30.4756	29.7613	29.4294
SCSF											
0	0	10.5508	10.4321	10.1337	10.0250	9.6804	9.5820	9.1545	9.0672	8.5376	8.4622
100	0	14.7632	14.6683	14.4651	14.3784	14.1476	14.0692	13.7878	13.7181	13.3783	13.3177
0	100	31.9301	31.7045	31.6123	31.3939	31.2587	31.0473	30.8351	30.6303	30.3138	30.1147
100	100	33.0947	32.8484	32.7640	32.5243	32.3938	32.1604	31.9469	31.7191	31.3915	31.1679
SSSF											
0	0	9.7169	9.6343	9.3327	9.2569	8.9153	8.8464	8.4309	8.3695	7.8627	7.8094
100	0	13.8568	13.7957	13.5806	13.5246	13.2850	13.2340	12.9475	12.9017	12.5585	12.5179
0	100	28.5963	28.4295	28.2364	28.0682	27.8271	27.6565	27.3231	27.1487	26.6817	26.5012
100	100	29.4798	29.2912	29.0924	28.9018	28.6498	28.4562	28.1020	27.9039	27.4015	27.1968
SFSF											
0	0	8.0095	7.9631	7.6928	7.6503	7.3487	7.3102	6.9495	6.9153	6.4811	6.4516
100	0	10.1228	10.8073	9.8115	10.8073	9.4690	10.8073	9.0652	9.8057	8.5817	9.1624
0	100	14.6514	14.4046	14.2177	13.9811	13.7364	13.5110	13.1641	12.9520	12.4725	12.2765
100	100	14.7374	14.4844	14.2963	14.0542	13.8072	13.5770	13.2263	13.0101	12.5252	12.3258

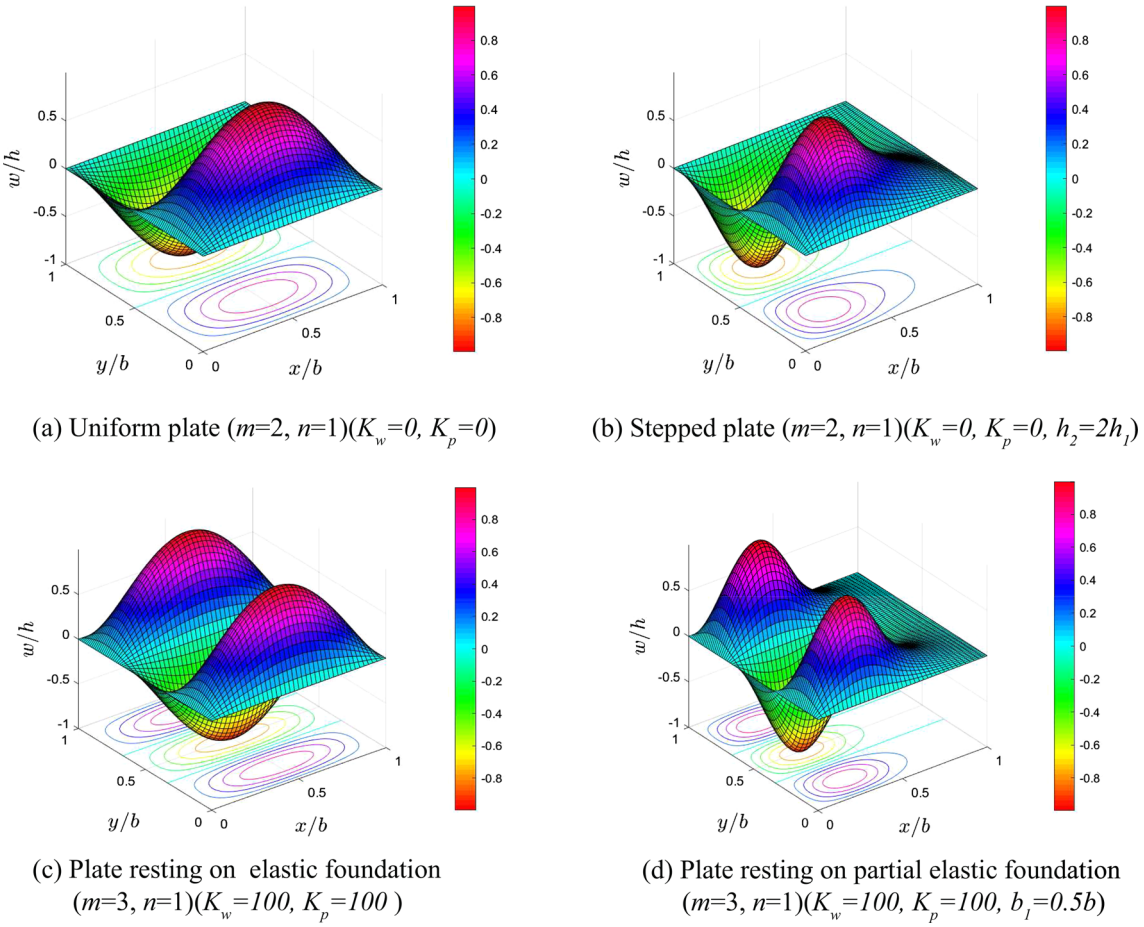

(a) Uniform plate (m=2, n=1)(K_w=0, K_p=0)

(b) Stepped plate (m=2, n=1)(K_w=0, K_p=0, h_2=2h_1)

(c) Plate resting on elastic foundation (m=3, n=1)(K_w=100, K_p=100)

(d) Plate resting on partial elastic foundation (m=3, n=1)(K_w=100, K_p=100, b_1=0.5b)

Fig. 10 Modeshapes of different configurations of square S-FGM plates: **a** uniform plate without elastic foundation, **b** stepped plate without elastic foundation ($h_2 = 2h_1$), **c** plate resting on homogeneous elastic foundation ($b_1 = 0.5b$), and **d** plate resting on non-homogeneous elastic foundation. ($L = b,\ \ h = 0.05b,\ \ p = 2$)

of the stepped plate with $h_2 = 2h_1$. Evidently, the peak of the modeshape plot of the stepped plate (i.e., Fig. 10b) has shifted to the left side the plate. This shift is attributed to the increased plate thickness, at the right half of the plate, which introduces greater resistance against bending. Figure 10c and d shows the modeshape of the uniform thickness plate resting on homogeneous and non-homogeneous elastic foundation, respectively. The effect of partial elastic foundation on the modeshape of the plate can be clearly seen in Fig. 10c where the peak of modeshape plot of the plate has been shifted toward the unsupported portion of the plate.

6 Conclusions

This study presents the exact formulation of the dynamic stiffness matrix for the free vibration analysis of S-FGM plate supported on elastic foundation. The distribution of material properties in the thickness of the S-FGM plate is defined using two separate power-law distribution for the two half of the plate which is normally called as sigmoid-law (S-FGM) property distribution. The effective elastic properties are estimated using the rule of mixture. The dynamic stiffness method is applied for two cases where the plate kinematic variables are defined for one case using CPT and for the other case using FSDT. For both these cases, the frequency-dependent dynamic stiffness matrix gives rise to the transcendental eigenvalue problem, which is solved by using the Wittrick and Williams algorithm.

It can be emphasized that the present DSM computed results, for the S-FGM plate resting on elastic foundation, are compared with the available results and an excellent agreement has been found. One important contribution of the present study is that it points out some incorrect mathematical formulation in a recently

published paper [18] and discusses all the possible mistakes in detail. It is also shown that the error in the frequency computation in that paper is as high as 34 %. Therefore, the present paper serves as correction to the work presented in [18]. The present work further enhances the previously published work by implementing a FSDT-based dynamic stiffness formulation for the elastically supported S-FGM plates. As FSDT considers the effect of transverse shear, the reported results will be applicable to thin as well as moderately thick FGM plates.

Furthermore, a thorough parametric analysis of fundamental frequencies influenced by power-law exponent, plate aspect ratios, and elastic foundation stiffness parameters is performed. From this analysis, several inferences are made using different tables and line diagrams. From the reported results, it can be seen that Pasternak foundation adds more restraint to bending compared to the Winkler foundation. This is because, unlike the Winkler model, which consists of independent and unconnected springs, the Pasternak foundation introduces a shear layer that accounts for both longitudinal and transverse spring effects. Furthermore, comparison of the two non-uniform configurations, considered in the study, shows that the introduction of stepped thickness enhances the frequency values. However, the frequency increase due to the presence of partial Pasternak foundation remains higher than that of the stepped plate as the Pasternak foundation provides a very high stiffness due to the presence of the shear layer. Lastly, it is reemphasized that, due to the exact mathematical formulation, the natural frequencies obtained using DSM are considered to be very accurate and these results can be used as a benchmark for future design purposes.

Author contribution RK helped in conceptualization, data curation, formal analysis, investigation, methodology, validation, visualization, software, writing—original draft; PJ was involved in conceptualization, resources, supervision, writing—review & editing.

Data availability This paper has no associated data or the data will not be deposited. [Authors' comment: The work presents an theoretical study and no experimental data are available. For the theoretical data that support the findings of the present work can be available from the corresponding author on request.]

Declarations

Competing interest The authors declare that they have no known competing financial interests or personal relationships that could have appeared to influence the work reported in this paper.

Appendix A: Stress–strain constitutive relation

The stress–strain constitutive relation for the FGM plate is expressed as [36]:

$$\begin{bmatrix} \sigma_{xx} \\ \sigma_{yy} \\ \sigma_{xy} \end{bmatrix} \begin{bmatrix} Q_{11} & Q_{12} & 0 \\ Q_{12} & Q_{22} & 0 \\ 0 & 0 & Q_{66} \end{bmatrix} \begin{bmatrix} \varepsilon_{xx} \\ \varepsilon_{yy} \\ \gamma_{xy} \end{bmatrix}. \tag{A.1}$$

In addition we will have,

$$\sigma_{yz} = Q_{44}\gamma_{yz} \text{ and } \sigma_{xz} = Q_{55}\gamma_{xz} \tag{A.2}$$

The reduced stiffness components are expressed in terms of material constants, written as:

$$\begin{aligned} Q_{11} = Q_{22} = \frac{E(z)}{1-\mu^2}; \quad Q_{12} = \frac{\mu E(z)}{1-\mu^2}; \\ Q_{44} = Q_{55} = Q_{66} = \frac{E(z)}{2(1+\mu)}. \end{aligned} \tag{A.3}$$

Appendix B: Expression for bending stiffness and inertia term

$$\begin{aligned} I_0 = \int_{-h/2}^{h/2} \rho(z)\mathrm{d}z; \quad I_2 = \int_{-h/2}^{h/2} (z-z_0)^2 \rho(z)\mathrm{d}z, \\ D_{\mathrm{sfgm}} = \int_{-h/2}^{h/2} (z-z_0)^2 Q_{11}(z)\mathrm{d}z; \quad \widehat{A_s} = \int_{-h/2}^{h/2} k_s Q_{44}(z)\mathrm{d}z. \end{aligned} \tag{B.1}$$

Here, k_s (= 5/6) is the shear correction factor [43];

Appendix C: Explicit expressions of Λ_i and Γ_i

Mathematical expression of Λ_i and Γ_i with $i = 1, 2, 3$, used in Eq. (45), is given below.

$$\begin{aligned}
\Lambda_i &= (\widehat{A_s}(-2\widehat{A_s} + 2I_2\omega^2 + D_{\text{sfgm}}(-1+\mu)(\alpha_m - m_i)(\alpha_m + m_i)))/(m_i(2A_s^2 \\
&\quad - A_s D_{\text{sfgm}}(1+\mu)(\alpha_m - m_i)(\alpha_m + m_i) + D_{\text{sfgm}}(1+\mu)(-\alpha_m^2 k_p - k_w + I_0\omega^2 + k_p m_i^2))), \\
\Gamma_i &= (\alpha_m m_i(2\widehat{A_s}^2 - \alpha_m^2 \widehat{A_s} D_{\text{sfgm}}(1+\mu) - D_{\text{sfgm}}(1+\mu)(\alpha_m^2 k_p + k_w - I_0\omega^2) + D_{\text{sfgm}}(\widehat{A_s} \\
&\quad + k_p)(1+\mu)m_i^2))/(2\alpha_m^4 D_{\text{sfgm}}(\widehat{A_s} + k_p) + \alpha_m^2(2(\widehat{A_s}k_p + D_{\text{sfgm}}k_w - (D_{\text{sfgm}}I_0 \\
&\quad + I_2(\widehat{A_s} + k_p))\omega^2) + D_{\text{sfgm}}(\widehat{A_s} + k_p)(-3+\mu)m_i^2 - (-k_w + I_0\omega^2 + (\widehat{A_s} + k_p)m_i^2)(2\widehat{A_s} \\
&\quad - 2I_2\omega^2 + D_{\text{sfgm}}(-1+\mu)m_i^2)).
\end{aligned} \tag{C.1}$$

References

1. Koizumi, M.: FGM activities in Japan. Compos. B Eng. **28**, 1–4 (1997)
2. Shiota, I., Miyamoto, Y.: Functionally Graded Materials. Elsevier, Amsterdam (1997)
3. Birman, V., Byrd, L.: Modeling and analysis of functionally graded materials and structures. Appl. Mech. Rev. **60**(5), 195–216 (2007)
4. Turan, M.: Bending analysis of two-directional functionally graded beams using trigonometric series functions. Arch. Appl. Mech. **92**, 1841–1858 (2022)
5. Suresh, S., Mortensen, A.: Functionally graded metals and metal-ceramic composites: part 2 thermomechanical behaviour. Int. Mater. Rev. **42**, 85–116 (1997)
6. Udupa, G., Rao, S.S., Gangadharan, K.V.: Functionally graded composite materials: an overview. Procedia Mater. Sci. **5**, 1291–1299 (2014)
7. Jha, D.K., Kant, T., Singh, R.K.: A critical review of recent research on functionally graded plates. Compos. Struct. **96**, 833–849 (2013)
8. Praveen, G.N., Reddy, J.N.: Nonlinear transient thermoelastic analysis of functionally graded ceramic-metal plates. Int. J. Solids Struct. **35**(33), 4457–4476 (1998)
9. Zenkour, A.M.: A comprehensive analysis of functionally graded sandwich plates: part 2-buckling and free vibration. Int. J. Solids Struct. **42**(18–19), 5243–5258 (2005)
10. Kumar, S., Ranjan, V., Jana, P.: Free vibration analysis of thin functionally graded rectangular plates using the dynamic stiffness method. Compos. Struct. **197**, 39–53 (2018)
11. Kumar, R., Jana, P.: Free vibration analysis of uniform thickness and stepped P-FGM plates: a FSDT-based dynamic stiffness approach. In: Mechanics Based Design of Structures and Machines (2022)
12. Thang, P.T., Nguyen-Thoi, T., Lee, J.: Closed-form expression for nonlinear analysis of imperfect sigmoid-FGM plates with variable thickness resting on elastic medium. Int. J. Mech. Sci. **143**, 143–150 (2016)
13. Lee, C.Y., Kim, J.H.: Evaluation of homogenized effective properties for FGM panels in aero-thermal environments. Compos. Struct. **120**, 442–450 (2015)
14. Kumar, S., Jana, P.: Application of dynamic stiffness method for accurate free vibration analysis of sigmoid and exponential functionally graded rectangular plates. Int. J. Mech. Sci. **163**, 105105 (2019)
15. Ootao, Y., Tanigawa, Y.: Three-dimensional solution for transient thermal stresses of functionally graded rectangular plate due to nonuniform heat supply. Int. J. Mech. Sci. **47**(11), 1769–1788 (2005)
16. Reddy, K.S.K., Kant, T.: Three-dimensional elasticity solution for free vibrations of exponentially graded plates. J. Eng. Mech. **140**, 7, 04014047 (2014)
17. Chi, S.H., Chung, Y.L.: Mechanical behavior of functionally graded material plates under transverse load-part II: numerical results. Int. J. Solids Struct. **43**(13), 3675–3691 (2006)
18. Chauhan, M., Dwivedi, S., Jha, R., Ranjan, V., Sathujoda, P.: Sigmoid functionally graded plates embedded on Winkler–Pasternak foundation: free vibration analysis by dynamic stiffness method. Compos. Struct. **288**, 115400 (2022)
19. Chonan, S.: Random vibration of an initially stressed thick plate on an elastic foundation. J. Sound Vib. **71**(1), 117–127 (1980)
20. Xiang, Y.: Vibration of rectangular Mindlin plates resting on non-homogenous elastic foundations. Int. J. Mech. Sci. **45**(6–7), 1229–1244 (2003)
21. Wang, T.M., Stephens, J.E.: Natural frequencies of Timoshenko beams on Pasternak foundations. J. Sound Vib. **51**(2), 149–155 (1977)
22. Zhang, D.G.: Nonlinear bending analysis of FGM rectangular plates with various supported boundaries resting on two-parameter elastic foundations. Arch. Appl. Mech. **84**, 1–20 (2014)
23. Xiang, Y., Wang, C.M., Kitipornchai, S.: Exact vibration solution for initially stressed Mindlin plates on Pasternak foundations. Int. J. Mech. Sci. **36**(4), 311–316 (1994)
24. Lam, K.Y., Wang, C.M., He, X.Q.: Canonical exact solutions for Levy-plates on two-parameter foundation using Green's functions. Eng. Struct. **22**(4), 364–378 (2000)

25. Malekzadeh, P., Karami, G.: Vibration of non-uniform thick plates on elastic foundation by differential quadrature method. Eng. Struct. **26**(10), 1473–1482 (2004)
26. Baferani, A.H., Saidi, A.R., Ehteshami, H.: Accurate solution for free vibration analysis of functionally graded thick rectangular plates resting on elastic foundation. Eng. Struct. **93**(7), 1842–1852 (2011)
27. Jung, W.Y., Han, S.C., Park, W.T.: Four-variable refined plate theory for forced-vibration analysis of sigmoid functionally graded plates on elastic foundation. Int. J. Mech. Sci. **111**, 73–87 (2016)
28. Omurtag, M.H., Özütok, A., Aköz, A.Y., Özcelikörs, Y.: Free vibration analysis of Kirchhoff plates resting on elastic foundation by mixed finite element formulation based on Gateaux differential. Int. J. Numer. Methods Eng. **40**(2), 295–317 (1997)
29. Zhou, D., Cheung, Y.K., Lo, S.H., Au, F.T.K.: Three-dimensional vibration analysis of rectangular thick plates on Pasternak foundation. Int. J. Numer. Methods Eng. **59**(10), 1313–1334 (2004)
30. Malekzadeh, P., Karami, G.: A mixed differential quadrature and finite element free vibration and buckling analysis of thick beams on two-parameter elastic foundations. Appl. Math. Model. **32**(7), 1381–1394 (2008)
31. Banerjee, J.: Dynamic stiffness formulation for structural elements: a general approach. Comput. Struct. **63**, 101–103 (1997)
32. Banerjee, J., Papkov, S., Liu, X., Kennedy, D.: Dynamic stiffness matrix of a rectangular plate for the general case. J. Sound Vib. **342**, 177–199 (2015)
33. Jun, L., Yuchen, B., Peng, H.: A dynamic stiffness method for analysis of thermal effect on vibration and buckling of a laminated composite beam. Arch. Appl. Mech. **87**, 1295–1315 (2017)
34. Kumar, R., Jana, P.: Exact modal analysis of multilayered FG-CNT plate assemblies using the dynamic stiffness method. In: Mechanics of Advanced Materials and Structures (2022)
35. Boscolo, M., Banerjee, J.: Dynamic stiffness elements and their applications for plates using first order shear deformation theory. Comput. Struct. **89**, 395–410 (2011)
36. Boscolo, M., Banerjee, J.: Dynamic stiffness formulation for composite Mindlin plates for exact modal analysis of structures. Part I: theory. Comput. Struct. **96**, 61–73 (2012)
37. Wittrick, W., Williams, F.: A general algorithm for computing natural frequencies of elastic structures. Q. J. Mech. Appl. Math. **24**, 263–284 (1971)
38. Wittrick, W., Williams, F.: Buckling and vibration of anisotropic or isotropic plate assemblies under combined loadings. Int. J. Mech. Sci. **16**, 209–239 (1974)
39. Larbi, L.O., Kaci, A., Houari, M.S.A., Tounsi, A.: An efficient shear deformation beam theory based on neutral surface position for bending and free vibration of functionally graded beams. Mech. Based Des. Struct. Mach. **41**, 421–433 (2013)
40. Abrate, S.: Functionally graded plates behave like homogeneous plates. Compos. B Eng. **39**, 151–158 (2008)
41. Saidi, A., Jomehzadeh, E.: On the analytical approach for the bending/stretching of linearly elastic functionally graded rectangular plates with two opposite edges simply supported. Proc. Inst. Mech. Eng. C J. Mech. Eng. Sci. **223**, 2009–2016 (2009)
42. Chauhan, M., Dwivedi, S., Mishra, P., Ragulskis, M., Burdzik, R., Ranjan, V.: Exponential functionally graded plates resting on Winkler–Pasternak foundation: free vibration analysis by dynamic stiffness method. Arch. Appl. Mech. **93**, 2483–2509 (2023)
43. Reissner, E.: On the theory of bending of elastic plates. J. Math. Phys. **23**(1–4), 184–191 (1944)